nature portfolio

Peer Review File

Nonlinear cascaded quantum network with giant emitters

Corresponding Author: Professor Xin Wang

This file contains all reviewer reports in order by version, followed by all author rebuttals in order by version.

Attachments originally included by the reviewers as part of their assessment can be found at the end of this file.

Version 0:

Reviewer comments:

Reviewer #1

(Remarks to the Author)
Comments are in the attached report.

Reviewer #2

(Remarks to the Author)
This paper presents a scheme of directional generation of multiple-photon bound states using nonlinear waveguides of photons and giant emitters (GEs) that couple to different sites of the waveguide with different phases. The key ideas are: (1) bound states of multiple photons (in particular, dublons for two photons) are formed with center-of-mass momentum K; (2) Lower-photon emissions (such as single-photon emission) are virtual and can be adiabatically eliminated by setting the parameters such that the bound states of interest are within the gaps between the energy bands for the scattering states of different numbers of photons; (3) GEs have different pathways to generate the multi-photon bound states with c.o.m momentum K or -K (by energy conservation under the Markovian approximation for the dublon emission) and the interferenece between such pathways of emission, whose phases depend on c.o.m. momentum and the sites where the photon emission occurs, leads to the direction selection (K versus -K), defined as chirality C. A toy model consisting of a tight-binding 1D chain of cavities with on-site interaction (Hubbard type U) and two-level GEs each coupled to two cavities separated by distance d (=0, 1, etc). It is understandable such a simple model is empployed for a proof-of-the-principle study. The calculation shows that the chirality C in a quite large range of parameters is close to the perfect values +/- 1. The physics behind the calculation is well understood. The authors present a scheme of cascade quantum networks based on the directional generation of photon doublons. The scheme can be generalized to more-photon bound state. A scheme of generating multi-atom NOON state is also presented. Using realistic parameters of suoerconducting resonator systems that are currently available in laborratories, the authors demonstrate the feasibility of the schemes. The paper in general is clearly written. I recommend the acceptance of the paper after addressing the following points (some are quite minor):

1. There are existing schemes of generating directional single photons or photons in coherent states using superradiance of atom ensembles (time-Dicked states), which can be understood as one-photon generating GE in some sense [see, e.g., PRA 91, 011801(R) (2015)]. For single photon states, of course, the nonlinear interaction between photons is not needed. Such literature should be introduced.

2. In Eq. (2) and some other places, r (deinfed as m-n) is used to refer to the relative distance between two photons. But in most places of the paper, r_d is used (even including in Eq. (2)). The symbol should be unified.

3. Persentation of Fig. 2 is not clear enough. Fig. 2a needs more explaining - what are bars? What are the shadowed curves? Are are (1) and (2) and the arrows? In Fig. 2b, what is c_{x_c r_d} (t) (not defined)? What is the value of time t in the plot (since in the figure c is plot as a function of x_c and r_d, not t)? In Fig. 2d, what is the value of \Delta_e (there are two in Fig. 2b & 2c)?

4. C should be a predic function of \Phi^e_1 and \Phi_e_2. Why does C change its sign when \Phi^e_{1/2} change from -pi to +pi (increased by 2\pi) as shown in the diagonal regions in Fig. 2d?

5. Does the optimal \Delta_e depend on d (the size of a GE)? If yeas, what is the value of \Delta_e in Fig. s4 (which shows

the dependence of chirality C on d)? Is it the same for all d's or optimized for each d?

6. In Eq. (19), the decay rates are temporally modulated to optimize state transfer between different sites. Ref. [8] is cited for this. There were earlier works proposing such ideas, see, e.g., PRL 78, 3221 (1997) and PRL 95, 030504 (2005), which may be appropriate references.

Reviewer #3

(Remarks to the Author)
In "Nonlinear cascaded quantum network with giant emitters" Wang et al. propose to combine giant emitters with nonlinear waveguides as a way to obtain directional emission of mutiphoton bound states for quantum network applications. As possible applications, they propose the long-distance transfer of an entangled Bell state and or the dissipative generation of multipartite entanglement. They briefly discuss the feasability of an implementation in circuit QED.

In my view, the present work builds upon the photon bound-state emission analysis presented in Ref. [49], employing the same approximations and arriving at an almost identical mathematical description of the emission process. The key difference is that, in the current case, the emission can be directional. This arises from the use of giant atoms, which couple to neighboring nodes with different phases—an effect that has been extensively studied in the literature on linear waveguides. The combination of this directionality (introduced by giant atoms) and the same approximations used in the master-equation derivation of Ref. [49] leads to a cascaded master equation involving multiple emitters. The authors identify this equation as equivalent to those previously shown to support remarkable applications in cascaded networks within linear waveguides, such as state transfer and entanglement distribution.

Clarity: The combination of these two setups—nonlinear waveguides and giant atoms—requires the reader to grasp two conceptually nontrivial ideas. However, the manuscript devotes only a very limited amount of space to explaining them. As a result, the paper could be made significantly clearer and easier to follow if the authors expanded these sections and provided a more detailed discussion of the underlying concepts.

Novelty and relevance: I find the idea of combining giant atoms with nonlinear waveguides novel and potentially interesting. However, its relevance to the field of quantum networks is not at all clear. To the best of my knowledge, directional emission of correlated photons can already be achieved using linear waveguides. For example, this can be realized with two directly interacting emitters, or with a single emitter possessing multiple energy levels or enabling two-photon transitions. It would therefore be important for the authors to clarify what specific advantages from introducing nonlinear waveguides, as opposed to the well-studied linear systems that already support cascaded quantum networks.

Leaving aside this major point, I have a few additional comments and questions:

-Can the choice of phases be adjusted to recover the non-directional emission discussed in Ref. [49]? Addressing this point (for example, in page 4 when directional emission is introduced) would help strengthen the conceptual link between the present results and those of Ref. [49].

-What is the main source of imperfection that limits the reported fidelity to 98%, rather than 100%?

-The use of the term “intriguing” in this context does not seem appropriate for a scientific manuscript, in my opinion. A more precise and descriptive characterization of the result would be preferible.

-The paragraph on experimental feasibility appears to closely follow that of Ref. [49], suggesting that an independent evaluation may not have been performed. It would be useful if the authors could comment on the coupling strengths (g values) reported in the cited giant-atom experiments and discuss whether these are consistent with the parameters used in their simulations.

Version 1:

Reviewer comments:

Reviewer #1

(Remarks to the Author)
I would like the authours for providing the asked clarifications. I would recommend the article for publication in its current form.

Reviewer #2

(Remarks to the Author)
The authors have addressed all the comments of the reviewers. I recommend the publication of the paper as is.

Reviewer #3

(Remarks to the Author)
I believe that the authors’ responses to two of my previous queries require further clarification and substantive improvement. In addition, I have identified a new potential source of confusion in the manuscript.

- Entanglement transfer with linear waveguides -

To my comment on the novelty and relevance, the authors respond that "conventional methods are limited to transfer one excitation at a time". However, they also say "As the Reviewer rightly notes, directional emission of single photons or correlated (I assume multiphoton?) photons can indeed be achieved in linear systems". These two statements appear internally inconsistent and require clarification.

If the authors believe that nonlinear waveguides provide an "alternative" route for entanglement state transfer in a single-step operation, then they should explicitly acknowledge and cite existing approaches based on linear waveguides that achieve comparable functionality, and clearly position their method as an alternative within this broader landscape. Conversely, if the authors claim that nonlinear waveguides constitute the only known approach (to the best of current knowledge) enabling entanglement state transfer in a single-step operation, this claim should be stated explicitly.

At present, the manuscript remains too vague on this point. For instance, the authors write: "Unlike conventional multipartite entanglement transfer with single flying qubits, this nonlinear interface enables entanglement state transfer in a single-step operation"

-Do linear waveguides support emission of two-photon states? If yes, then it seems that entanglement-transfer is also possible using linear waveguides. For example Ref.[69] suggests that multi-photon emission is possible with linear waveguides.

-Also, it is not at all clear to me that single photons cannot be used for entanglement transfer. In quantum memories based on atomic ensembles, doesn't a single photon generate a multipartite entangled state in the atoms?

Similarly, the statement "Contrasting linear setups,..., our proposal utilizes supercorrelated photons as “flying qubits", enhancing numerous many-body applications" is too vague. The manuscript should explicitly identify which many-body applications are enhanced and explain how the use of supercorrelated photons provides a concrete advantage over linear-waveguide-based approaches.

- 98% fidelity -

In response to my question regarding the dominant sources of imperfection, the authors state that the error arises from (1) finite transfer time and (2) intermediate single-photon processes.

The authors should quantify the relative contributions of these two mechanisms to the reported 2% infidelity. In my understanding, the error associated with (1) can reduced by increasing the transfer time. In contrast, the imperfection arising from (2) seems more fundamental, as it is intrinsic to the dynamics and may require modification of system parameters or operating regimes to mitigate.

The manuscript would benefit from a discussion addressing how each error contribution can be reduced. For example, are there parameter regimes in which these intermediate single-photon processes are further suppressed ? Clarifying whether this source of imperfection sets a fundamental limit, or whether it can be engineered away, is essential for assessing the scalability and practical relevance of the proposal.

Also, I do not understand the use of the term "simulation" in "finite simulation time window". I understand the authors refer an error due to finite transfer time. This will also appear in real setups and does not have to do with specifics of the numerical simulation.

--- The dark state condition ---

"Because dark-state conditions always hold in this nonlinear cascaded system, the correlated-two-photon field is trapped between the two GEPs without leaking outside"

In the context of quantum-state transfer, modulation of the light-matter coupling is needed in order to satisfy a "dark state condition" and thus achieve perfect transfer. To state that "dark-state conditions always hold in this nonlinear cascaded system" is confusing since it suggests modulation is not needed to achieve perfect transfer.

RESPONSE LETTER TO REVIEWERS

Reviewer #1

Reviewer comments

The work by Wang et al (number COMMSPHYS-25-1042-T) studies the problem of two-legged giant atoms weakly- coupled to a non-linear homogeneous coupled cavity array, in which a boundphoton minibands exist regardless of the sign of the interaction. For instance, in case of two giant atoms (so called "giant emitter pair" GEP), both resonant to the mini-band, the authors discuss a mechanism for chiral emission of bound photon pairs, which is resilient to different geometric configurations of the giants, phase differences in the coupling etc. Building on that, together with technique of optimal control in time of the coupling strengths, the authors propose a so-called non-linear cascaded network, in which excitations can be deterministically transferred between different GEPs, or entanglement can be efficiently created between remote GEPs. In the end, the authors argue that this mechanism can be extended to configurations in which more than two photons are involved and discuss potential implementations within the paradigm of circuit-QED.

Our reply: We thank the Reviewer for giving a comprehensive summary of our work.

Reviewer comments

While the idea is potentially interesting, bridging non-linear systems with waveguide-QED, I cannot recommend it for publication before the authors have addressed the following points.

Our reply: Thank the Reviewer for recognizing the potential interest of our work. We appreciate the opportunity to address the concerns raised and have carefully revised the manuscript accordingly. Below, we provide a point-by-point response to the reviewer's comments.

Reviewer comments

1. When introducing the model of a non-linear coupled cavity array, the authors discuss and derive the dispersion law of the miniband of bound photons, see Eq. 5. This result though only holds when U<0 (attractive interaction), as correctly stated in the supplementary material. In general, since the sign of the interaction seems not to be so important for the discussed phenomenology, I would amend this part by including both solutions (or else justify why they need U<0 for everything to work).

Our reply: We sincerely thank the Reviewer for this insightful comment.

The wavefunction under repulsive interaction ($U > 0$) exhibits a notable sign alternation at nearest-neighbor r, which in turn influences the emitter's dynamics.

In response, we have added the following sentence in the main text (Page [2]) to clarify the main focus of our study:

Throughout this work, we focus on systems with attractive interactions $U < 0$. A detailed discussion of the repulsive case $U > 0$ is provided in Section I and II D of Supplementary Material.

Additionally, we have expanded the Supplementary Material to include further discussion on the repulsive case ($U > 0$):

1. In Sec. S I, we now provide the wavefunction for $U > 0$ and include a figure to visually compare the energy structure and wavefunctions for both $U > 0$ and $U < 0$.

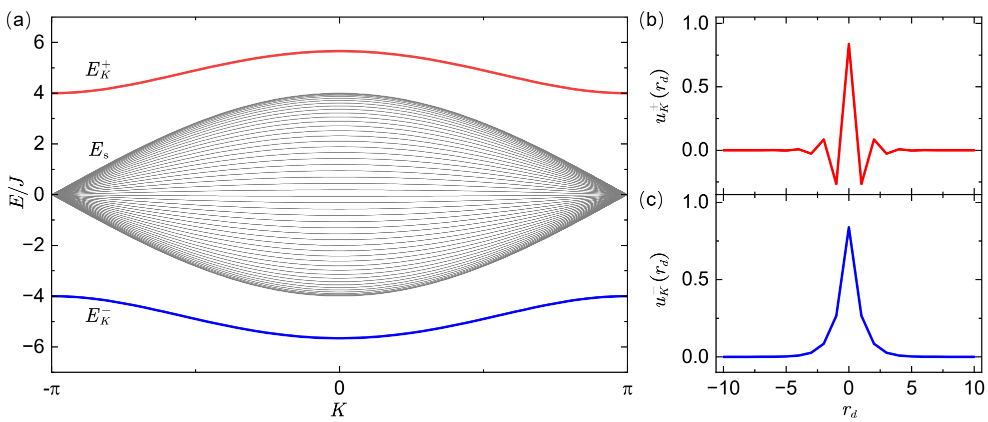

Figure R1. (a) Spectrum of the two-photon subspace. The bound states $E_K^{\pm}$ are given by Eqs. (S14) and (S15); while the scatter state is given by Eq. (S20). (b, c) Wavefunctions $u^{\pm}K(r_d)$ of the bound states at $K = \pi/2$, given by Eqs. (S16) and (S17). The superscript $\pm$ denotes the sign of the interaction U.

The wave function for mode K is written as

$$u_K(r_d) = \frac{G_K^0(E, r_d = 0)U}{1 - G_K^0(E, r_d = 0)U} G_K^0(E, r_d)$$
$$= \frac{G_K^0(E, r_d = 0)U}{1 - G_K^0(E, r_d = 0)U} \frac{1}{2\pi} \int dq \, \frac{e^{iqr_d}}{E + 4J\cos(\frac{K}{2})\cos q}.$$

Then, the wavefunction is written as [S1-S3]

$$U > 0, \quad u_K(r_d) = u_0(-1)^{|r_d|} \exp\left[-\frac{|r_d|}{L_u(K)}\right], \tag{R1}$$

$$U < 0, \quad u_K(r_d) = u_0 \exp\left[-\frac{|r_d|}{L_u(K)}\right], \tag{R2}$$

where u_0 is a normalization factor and the decay length for two-photon correlations in space is

$$L_u(K) = -\left[\ln\left(\frac{\sqrt{U^2+16J_K^2}-|U|}{4J_K}\right)\right]^{-1}, \tag{R3}$$

with $J_K = J\cos(K/2)$. Note that $L_u(K)$ rapidly decreases when increasing the nonlinear parameter U. Eventually, the wave function of the doublon state is written as

$$\Psi_{\mathrm{d}} = \frac{1}{\sqrt{2}}\sum_{m,n} e^{iK\frac{m+n}{2}} u_K(m-n). \tag{R4}$$

In Fig. S1, we plot the band structure $E_K^{\pm}$ versus K and the wavefunction $u_K^{\pm}(r_d)$ versus r_d at $K=\pi/2$. The superscript $\pm$ corresponds to the sign of the interaction U. The scattering state is plotted for reference [S3]

$$E_{\mathrm{s}} = -4J\cos(K/2)\cos(q), \tag{R5}$$

with relative momentum q.

We focus on the case $U<0$ throughout the article and a discussion of how $U>0$ affects these conclusions follows in the Sec. S II D.

2. We have added a new subsection titled "**D. Results for repulsive interaction** $U>0$" to systematically discuss the effects of repulsive interactions $U>0$.

D. Results for repulsive interaction $U > 0$

We now turn to the case of repulsive interaction $U>0$. By replacing the dispersion relation and the wavefunction in Eqs. (15) and (17) with those in Eqs. (16) and (18) throughout the derivation, we obtain the numerical and analytical results for $U>0$. Figure. S6 displays the decay rate Γ and the chiral factor C as functions of the phase $\Phi_{1,2}^e$ over an extended range of $[-2\pi, 2\pi]$, comparing repulsive ($U>0$) and attractive ($U<0$) interactions. Under a π-phase shift, the decay rate remains invariant, while the chirality is reversed due to the energy relation $E_K^{(U>0)} = -E_K^{(U<0)}$. To illustrate these dynamics, we present the time evolution and the photonic field distribution for two cases: (i) $U<0$, $\Delta_e<0$, $\Phi_{1,2}^e = -\pi/5$ and (ii) $U>0$, $\Delta_e>0$, $\Phi_{1,2}^e = -\pi/5+\pi = 4\pi/5$. These distinctive properties stem from the sign alternation of the wavefunction between nearest-neighbor r under repulsive ($U>0$), combined with the reversal of the dispersion relation, as shown in Fig. S1.

We hope these revisions adequately address the Reviewer's valuable point and improve the clarity and completeness of the manuscript.

Reviewer comments

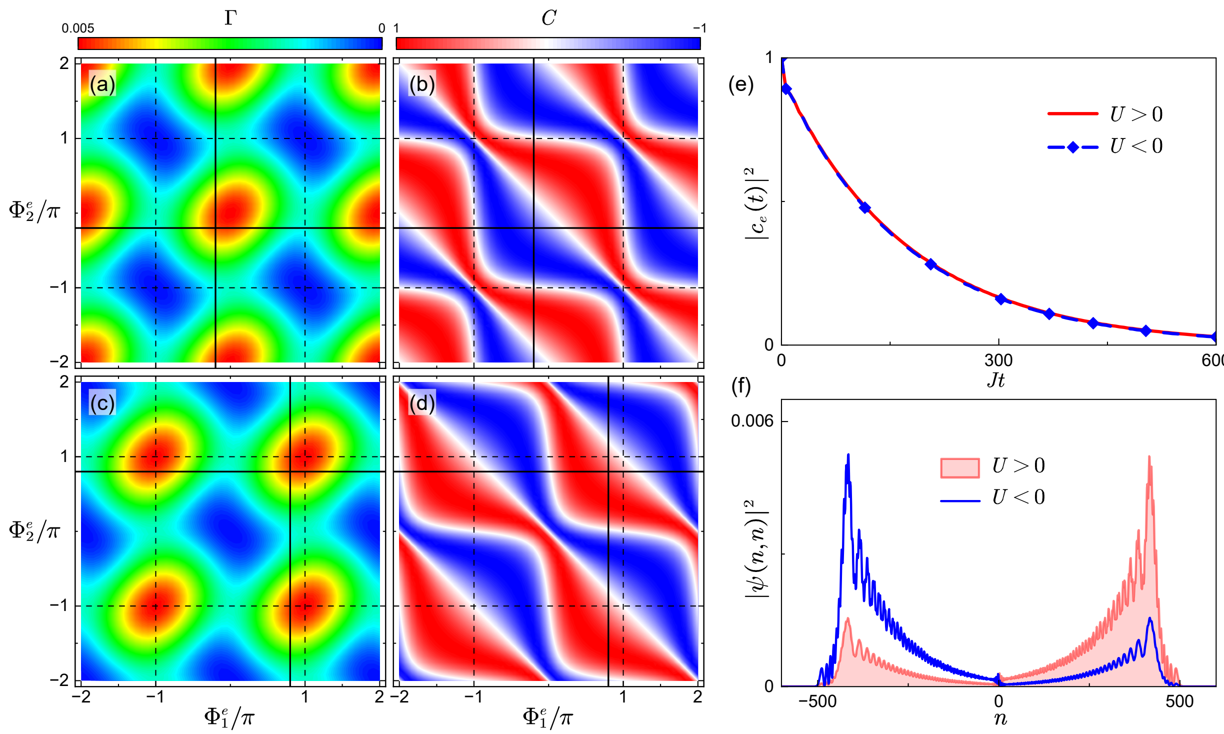

Figure R2. (a) Decay rate Γ and (b) chiral factor C as functions of $\Phi_1^(e)$ and $\Phi_2^(e)$ over $[-2\pi, 2\pi]$ for the attractive interaction $U < 0$. (c, d) Corresponding plots of Γ and C for the repulsive interaction $U > 0$. Dashed lines mark the first Brillouin zone boundaries. Solid lines indicate the parameter sets $\Phi_1^e, \Phi_2^e = -\pi/5$ (for $U < 0$) and $4\pi/5$ (for $U > 0$) used in (e) and (f). (e) Time evolution of $|c_e(t)|^2$. (f) Photonic field distribution $|\psi(n, n)|$ at $Jt = 600$. In (e) and (f), red curves correspond to $U > 0$, $\Delta_e > 0$, and $\Phi_{1,2}^e = 4\pi/5$; blue curves correspond to $U < 0$, $\Delta_e < 0$, and $\Phi_{1,2}^e = -\pi/5$. Parameters: $d = 1$, $g = 0.1J$, $|U| = 4J$, $2|\Delta_e| = 5.1J$.

2. Maybe I would omit the derivation of this dispersion relation as it does not compromise the readability of the paper, and there is already extensive literature showing how to derive those states e.g., J. Phys. B: At. Mol. Opt. Phys. 41 161002 (2008). Though, I leave this point with the authors' judgement.

Our reply: We thank the Reviewer for this valuable suggestion. The referenced work has now been cited in both the main text and the Supplementary Information. We put the detailed discussion of the repulsive case $U > 0$ in Supplementary Material Section I and II D (not shown in the main text).

Reviewer comments

3. I would ask the authors to simplify as much as possible the notation in this paper, as it really hinders the readability of the paper. For instance, I find the use of G^2 for the twophoton correlator a bit confusing since capital G is already used for the Green's function. Also, I *would suggest the authors checking whether there are symbols which are used in the main text yet not defined there. For example, after eq. 12 δ_k is not defined (and those equations lack the numbering) while being defined in the supplementary.*

Our reply:

We thank the Reviewer for the careful reading and the valuable feedback regarding notation clarity. We agree that consistent and clear notation is essential for readability, and we have taken the following steps to address the concerns raised:

1. **Simplification of redundant notation:**

   The quantities $f_K(n_1^\tau, n_2^\sigma)$ and $\vec{e}_{\tau\sigma}$ were previously defined separately but describe the same physical object. To avoid redundancy and improve clarity, we have removed the definition of $f_K(n_1^\tau, n_2^\sigma)$ entirely and now consistently use $\vec{e}_{\tau\sigma}$ throughout the main text and Supplement Information. On Page [3], the relevant section has been revised as follows:

   F_K is expressed as a sum over four decay channels:

   $$F_K = \sum_{\tau,\sigma} \vec{e}_{\tau\sigma}(K), \tag{R6}$$

   where each channel is represented as a complex vector to facilitate the interpretation of interference effects in subsequent sections. Each vector is defined as

   $$\vec{e}_{\tau\sigma}(K) = A_K\left(r_d^{\tau\sigma}\right) e^{i\phi_1^\tau} e^{i\phi_2^\sigma} e^{-iKx_c^{\tau\sigma}}, \tag{R7}$$

   with the amplitude

   $$A_K\left(r_d^{\tau\sigma}\right) = \sum_k \cos[(k - K/2) r_d^{\tau\sigma}] L_{k,K},$$
   $$L_{k,K} = \frac{2\sqrt{2}J}{N(\omega_k - \Delta_e)} \sum_m e^{-i(k-K/2)m} u_K(m),$$

   where $x_c^{\tau\sigma} = (n_1^\tau + n_2^\sigma)/2$, $r_d^{\tau\sigma} = n_1^\tau - n_2^\sigma$, $\delta_k = \omega_k - \Delta_e$ and $\omega_k = -2J\cos(k)$ is the single-photon dispersion relation.

   Accordingly, the original definitions in Eqs. (14) and (15) have been removed, and the surrounding text has been streamlined to maintain a clear logical progression.

2. **Explicit definition of previously undefined symbols:**

   - δ_k in $L_{k,K}$ is now defined after used:

     $\delta_k = \omega_k - \Delta_e$ and $\omega_k = -2J\cos(k)$ is the single-photon dispersion relation.

   - Δ_K in Eq. (10) is now defined after used:

     $\Delta_K = E_K - 2\Delta_e$

3. **Revised notation for the two-photon correlation function:**

   To prevent any potential confusion with the Green's function G, the two-photon spatial correlation function previously denoted as $G^{(2)}$ has been renamed as $\mathcal{G}^{(2)}$ throughout the text.

All relevant equations have also been properly numbered, and we have thoroughly verified that every symbol used in the main text is either defined or referenced clearly.

Reviewer comments

4. Eq. 16 is not trivial at all so I would ask to provide justification on its derivation

Our reply: We thank the Reviewer for this insightful comment. In the revised manuscript, we have expanded the logical derivation to enhance clarity. The key revisions are summarized as follows:

- **Introduction of the effective Hamiltonian for a single GEP:**

  We first explicitly present the effective interaction Hamiltonian for a single GEP on Page [3], following Eqs. (9) and (10). This establishes a clear physical foundation for extending the formalism to multiple GEPs.

  After adiabatically eliminating the single-photon intermediate state, we obtain the reduced two-photon state

$$|\psi(t)\rangle = \left[c_e(t)\sigma_1^+\sigma_2^+ + \sum_K c_K(t)\mathcal{D}_K^\dagger\right]|g, g, \text{vac}\rangle. \tag{R8}$$

  From Eqs. (9) and (10), the effective interaction Hamiltonian between GEP and the nonlinear waveguide, i.e., the state $|e, e, \text{vac}\rangle$ and $|g, g, K\rangle$ can be further derived as

$$H_{\text{int}} = \frac{g^2}{J}\sum_{\tau,\sigma}\sigma_1^-\sigma_2^-\mathcal{D}^\dagger_{n_1^\tau, n_2^\sigma} + \text{H.c.}, \tag{R9}$$

$$\mathcal{D}^\dagger_{n_1^\tau, n_2^\sigma} = \frac{1}{\sqrt{N_c}}\sum_K e^{i\Delta_K t} f_K(n_1^\tau, n_2^\sigma)\mathcal{D}_K^\dagger. \tag{R10}$$

  Note that, the operator $\mathcal{D}^\dagger_{n_1^\tau, n_2^\sigma}$ is defined in the interaction picture, which contains a time-depended phase factor.

- **Clarification of assumptions for the two-GEP network:**

  We then explicitly state the key assumptions for the two-GEP network: specifically, the separation condition $D_q \gg L_u(K)$, which suppresses supercorrelated radiation between emitters in different GEPs. Additionally, for the chosen initial state with only one GEP excited, we introduce the corresponding reduced two-photon state on Page [5].

We assume that the two GEPs have the same geometric layout but are separated by a distance D_q, with D_q sufficiently larger than $L_u(K_r)$. This ensures that supercorrelated emission between emitters in different pairs, i.e., the process $\langle \text{vac}|\mathcal{D}_K^\dagger \sigma_{\text{A},1/2}^- \sigma_{\text{B},1/2}^- |\text{vac}\rangle$, are suppressed. The operator $\sigma_{\alpha,i}^-$ denotes the lowering operator of emitter α_i. Under this condition, we consider the initial state:

$$|\psi(t=0)\rangle = \sigma_{\text{A},1}^+ \sigma_{\text{A},2}^+ |g, g, \text{vac}\rangle,$$

which only GEP A is excited, and states $\sigma_{\text{A},1/2}^- \sigma_{\text{B},1/2}^- |g, g, \text{vac}\rangle$ can be neglected. Accordingly, the reduced system state analogous to Eq. (13) becomes:

$$|\psi(t)\rangle = \left[\sum_\alpha c_e^\alpha(t) \sigma_{\alpha,1}^+ \sigma_{\alpha,2}^+ + \sum_K c_K(t) \mathcal{D}_K^\dagger\right] |g, g, \text{vac}\rangle. \tag{R11}$$

Here, $\alpha = \text{A, B}$ denotes that supercorrelated radiation is confined within individual GEPs.

- **Generalization to the two-GEP interaction Hamiltonian:**

  Building on the single-GEP result, we generalize the interaction Hamiltonian for the two-GEP network on Page [5]:

  Analogous to Eq. (14), the interaction Hamiltonian can be expanded in the basis of Eq. (17) as

  $$H_{\text{int}} = \frac{g^2}{J} \sum_\alpha \sum_{\tau,\sigma} \sigma_{\alpha,1}^- \sigma_{\alpha,2}^- \mathcal{D}^\dagger_{n^\tau_{\alpha,1}, n^\sigma_{\alpha,2}} + \text{H.c.} \tag{R12}$$

  In contrast to Eq. (14), the labels now include an additional index $\alpha = \text{A, B}$, where (α, i, τ) denotes the i-th emitter in pair α coupled to the waveguide at position $n^\tau_{\alpha,i}$

Reviewer comments

5. In eq. 17 the authors introduce a doublon state creation operator, which in the end is a time-dependent combination of what in the initial section were already called "doublons". I would ask the authors to clarify this point (also this dependency).

Our reply: We thank the Reviewer for careful reading and for identifying the imprecise description of the operator $\mathcal{D}^\dagger_{n_1^\tau, n_2^\sigma}$.

The operator $\mathcal{D}^\dagger_{n_1^\tau, n_2^\sigma}$ is not a doublon state creation operator. Instead, it is defined in the interaction picture and contains an explicit time-dependent phase factor $\exp i\Delta_K t$, where $\Delta_K = 2\Delta_e - E_K$ represents the frequency detuning. Consequently, referring to it as a "**doublon creation operator**" was inaccurate and potentially misleading.

To address this, we have made the following revisions to the manuscript:

1. We have removed the term "doublon creation operator" in reference to $\mathcal{D}^\dagger_{n_1^\tau, n_2^\sigma}$ and now refer to it simply as an operator.

2. We now introduce this operator earlier in the text, on Page [3] alongside Eqs. (9) and (10), as part of the derivation of the effective Hamiltonian for a single GEP, which clarifies its physical origin and mathematical form.

The revised description now reads:

Note that, the operator $\mathcal{D}^{\dagger}_{n_1^{\tau},n_2^{\sigma}}$ is defined in the interaction picture, which contains a time-depended phase factor.

We hope this clarification eliminate the ambiguity.

Reviewer comments

6. Given the analogy with the results of Ref. S5 (in Supp. Mat.), I would ask the authors to briefly comment on analogies and differences between their proposal and the standard system in which, through proper time-dependent couplings, a single excitation can be deterministically transferred between different atoms. What could be an advantage of using the proposed setup (if there is any)?

Our reply:

We sincerely thank the Reviewer for raising this insightful question.

While both our protocol and the scheme in Ref. S5 [PRA 84, 042341 (2011)] utilize properly engineered time-dependent couplings to mediate excitation transfer, they are distinct in physical mechanism: conventional protocols employ single photons as information carriers, whereas our approach exploits doublons (two-photon bound states) to enable **joint two-excitation transfer**. This key difference allows our setup to transfer two-photon (two-qubit) quantum states between remote network nodes in **a single-step operation**, in contrast to standard methods, which are limited to transferring one excitation (one qubit) at a time.

This capability is particularly advantageous for distributing multi-emitter entangled states. For example, in existing protocols, such as *Deterministic multi-qubit entanglement in a quantum network* [Fig. 3, adopted from Nature 590, 571 (2021)] **transferring a 3-qubit GHZ state requires three sequential single-qubit transfer operations, together with plenty of local gate operations.** By contrast, our architecture, where two emitters per node collectively couples to a nonlinear waveguide, enables **entanglement state transfer in a single-step operation**. Thus, a two-qubit entangled state prepared at node A, such as

$$|\Psi_{\mathrm{A}}(t_0)\rangle = c_e^{\mathrm{A}}|e,e\rangle + c_g^{\mathrm{A}}|g,g\rangle,$$

can be mapped onto node B in a single step, preserving entanglement without intermediate operations.

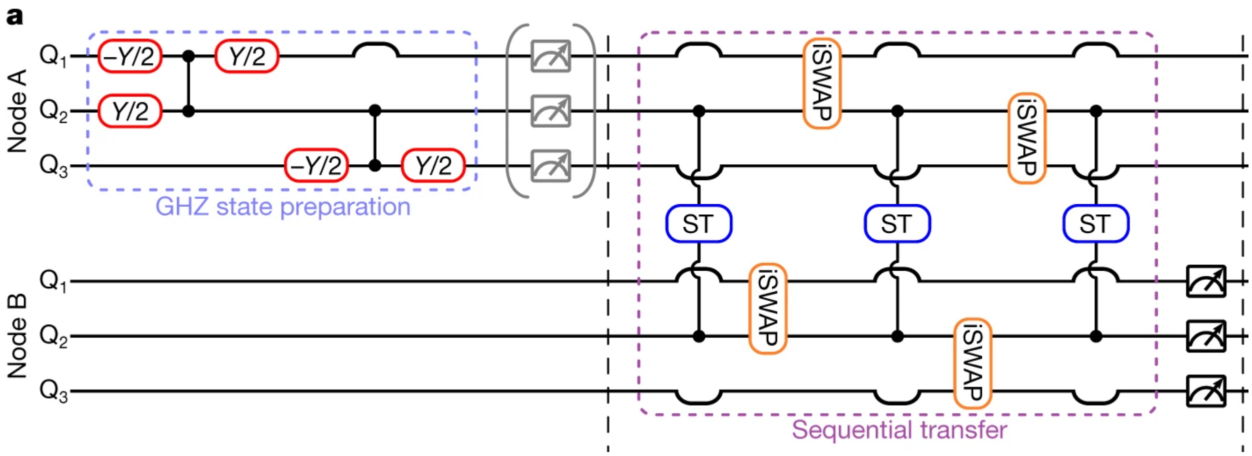

Figure R3. Schematic of the GHZ state preparation and the sequential state-transfer (ST) protocol in *Deterministic multi-qubit entanglement in a quantum network*. The figure is taken from *Nature 590, 571 (2021)*.

We have clarified this distinction on Page [6] of the revised manuscript by adding *Nature 590, 571 (2021)* as Ref [71]:

Unlike conventional multipartite entanglement transfer with single flying qubits [71], this nonlinear interface enables entanglement state transfer in a single-step operation. For example, an initial entangled state of GEP A, $|\Psi_{\rm A}(t_0)\rangle = c_e^{\rm A}|e,e\rangle + c_g^{\rm A}|g,g\rangle$, can be directly mapped onto GEP B as $|\Psi_{\rm B}(t_0)\rangle = c_e^{\rm B}|e,e\rangle + c_g^{\rm B}|g,g\rangle$ without sequential operations.

Reviewer comments

Minor comments 7. There are some typos: "direcional" on page 3, G^2 on Fig 4 caption etc

Our reply:

Thank the Reviewer for careful reading and for pointing out these typos. We have revised all of them.

Reviewer #2

Reviewer comments

This paper presents a scheme of directional generation of multiple-photon bound states using nonlinear waveguides of photons and giant emitters (GEs) that couple to different sites of the waveguide with different phases. The key ideas are: (1) bound states of multiple photons (in particular, dublons for two photons) are formed with center-of-mass momentum K; (2) Lower-photon emissions (such as single-photon emission) are virtual and can be adiabatically eliminated by setting the parameters such that the bound states of interest are within the gaps between the energy bands for the scattering states of different numbers of photons; (3) GEs have different pathways to generate the multi-photon bound states with c.o.m momentum K or -K (by energy conservation under the Markovian approximation for the dublon emission) and the interferenece between such pathways of emission, whose phases depend on c.o.m. momentum and the sites where the photon emission occurs, leads to the direction selection (K versus -K), defined as chirality C. A toy model consisting of a tight-binding 1D chain of cavities with on-site interaction (Hubbard type U) and two-level GEs each coupled to two cavities separated by distance d (=0, 1, etc). It is understandable such a simple model is empployed for a proof-of-the-principle study. The calculation shows that the chirality C in a quite large range of parameters is close to the perfect values +/- 1. The physics behind the calculation is well understood. The authors present a scheme of cascade quantum networks based on the directional generation of photon doublons. The scheme can be generalized to more-photon bound state. A scheme of generating multi-atom NOON state is also presented. Using realistic parameters of suoerconducting resonator systems that are currently available in laborratories, the authors demonstrate the feasibility of the schemes.

Our reply: We thank the Reviewer for giving a comprehensive summary of our work

Reviewer comments

The paper in general is clearly written. I recommend the acceptance of the paper after addressing the following points (some are quite minor):

Our reply: We sincerely thank the Reviewer for the positive assessment and for noting that the manuscript is clearly written. Below, we provide a point-by-point response to the Reviewer's comments and have revised the manuscript accordingly.

Reviewer comments

1. There are existing schemes of generating directional single photons or photons in coherent states using superradiance of atom ensembles (time-Dicked states), which can be understood as one-photon generating GE in some sense [see, e.g., PRA 91, 011801(R) (2015)]. For single photon states, of course, the nonlinear interaction between photons is not needed.

Such literature should be introduced.

Our reply:

We thank the Reviewer for pointing us to the relevant literature on directional single-photon generation via superradiance in atomic ensembles.

In response, we have added an introduction of generating directional single-photon research in the revised manuscript on Page [5].

Contrasting linear setups, such as interacting emitter pairs [6,7], multiple-level atoms [69], and superradiance of atom ensembles (time-Dicke states) [70], our proposal utilizes super-correlated photons as "flying qubits", enhancing numerous many-body applications.

Reviewer comments

2. In Eq. (2) and some other places, r (deinfed as $m - n$) is used to refer to the relative distance between two photons. But in most places of the paper, r_d is used (even including in Eq. (2)). The symbol should be unified.

Our reply:

We thank the Reviewer for careful reading and highlighting the inconsistency in notation. We have thoroughly revised the manuscript to ensure a unified notation throughout.

Specifically, we now consistently use $r_d = n_1 - n_2$ to denote the relative distance between two photons, while r is reserved for denoting the right coupling leg of giant emitters.

All relevant instances in the main text and Supplementary Material, including Eq. (2) and surrounding discussions, have been updated accordingly to ensure notational consistency and clarity.

Reviewer comments

3. Persentation of Fig. 2 is not clear enough. Fig. 2a needs more explaining - what are bars? What are the shadowed curves? Are are (1) and (2) and the arrows? In Fig. 2b, what is $c_{x_c,r_d}(t)$ (not defined)? What is the value of time t in the plot (since in the figure c is plot as a function of x_c and r_d, not t)? In Fig. 2d, what is the value of Δ_e (there are two in Fig. 2b & 2c)?

Our reply:

We thank the Reviewer for pointing out the ambiguities in the presentation of Fig. 2. We have thoroughly revised both the figure and its caption to improve clarity and address all the raised points. The specific revisions are as follows:

- **Fig. 2a**: The vertical bars represent a single photon emitted by one giant emitter at position n_1^l (n_2^r). The shaded curves depict the spatial profile of the intermediate single-photon state generated by the other emitter during the two-photon emission process. The symbols ① and ② denote the two giant emitters, which are coupled to the waveguide, as indicated by the black and red dashed arrows, respectively.

- **Fig. 2b**: The quantity $|c_{x_c,r_d}(t)|^2$ denotes the joint probability distribution of two photons with center-of-mass coordinate $x_c = (n_1 + n_2)/2$ and relative coordinate $r_d = n_1 - n_2$, where n_1 and n_2 are the lattice positions of two photons. The distribution is plotted at time $Jt = 600$, corresponding to the dashed vertical line in Fig. 2c, when the emitter population has largely decayed.

- **Fig. 2b**: The emitter detuning is set to $2\Delta_e = -5.1J$ (i.e., $\Delta_e = -2.55J$), which corresponds to the optimal condition for directional doublon emission, consistent with the parameters used in Fig. 2b.

All these clarifications have been incorporated into the revised caption of Fig. 2 on Page [4]

Directional emission of doublons. (a) Sketches of the dual transition processes described by $\vec{e}_{lr}$. Vertical bars indicate a single photon localized at n_1^l (n_2^r), while the shaded curves represent the spatial envelope of the intermediate single-photon state. Two giant emitters {①, ②} are coupled to the waveguide at positions marked by the black and red dashed arrows, respectively. (b) Two-photon joint probability distribution $|c_{x_c,r_d}(t)|^2$ at time $Jt = 600$ (dashed line in c) with $2\Delta_e = -5.1J$ (optimal emission point). $x_c = (n_1 + n_2)/2$ and $r_d = n_1 - n_2$ denote the center-of-mass and relative coordinates of two photons at sites n_1 and n_2. The two-point correlation function $\mathcal{G}^{(2)}(r_d)$ is also shown. (c) Time evolution of $|c_e(t)|^2$ for $2\Delta_e = -4.6J$ and $-5.1J$. (d) Chiral factor as a function of $\Phi_{1,2}^e = \phi_{1,2}^r - \phi_{1,2}^l$, with $2\Delta_K = -5.1J$. The coupling strength is set to $g = 0.1J$; other parameters are the same as in Fig. 1d.

Reviewer comments

4. C should be a predic function of Φ_1^e and Φ_2^e. Why does C change its sign when $\Phi_{1/2}^e$ change from $-pi$ to $+pi$ (increased by 2π) as shown in the diagonal regions in Fig. 2d?

Our reply:

We thank the Reviewer for this insightful question. The chiral factor C is indeed a periodic function of Φ_1^e and Φ_2^e, with a period of 2π. To better illustrate this periodicity across multiple Brillouin zones, in Fig. R4, we plot C over an extended phase range $[-2\pi, 2\pi]$.

The sign reversal of C along the diagonal regions of Fig. 2d results from quantum interference among the four decay channels mediated by the GEP. To clarify this behavior and explicitly identify the parameter regions where $C = 0$, we have expanded Sec. S II C in Supplementary Material and added two new subsections (Sec. II C 2 and II C 3). These additions provide a

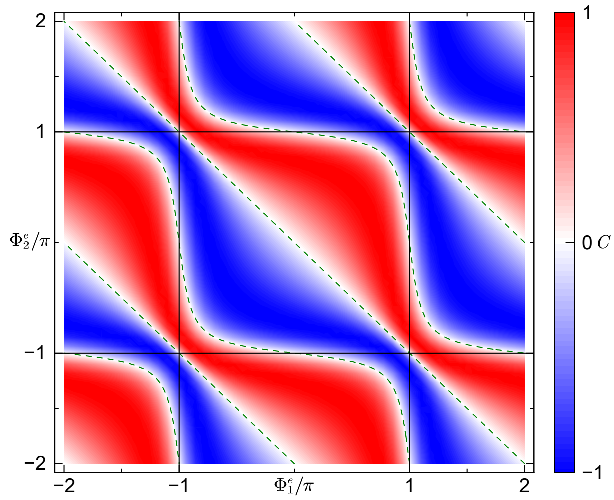

Figure R4. Chiral factor as a function of Φ_1^e and Φ_2^e, with $2\Delta_K = -5.1J$. The green dashed curves are given by (R22b) and (R22c). The coupling strength is set to $g = 0.1J$; other parameters are the same as in Fig. 2d.

detailed analytical treatment of how the sign of C is governed by Φ_1^e and Φ_2^e, and explicitly derive the nodal lines where the chiral factor vanishes.

C. Effects of the parameters of the GEP on decay and chiral

Equations (S45) and (S46) gives the analytical expressions of the decay rate and chiral factor, respectively. Leveraging these expressions, we now analyze how the geometric and coupling parameters of the GEP shape its dynamics.

2. Effects of the coupling phases and resonance frequency

We now focus on the case $D = 0$, and discuss how the coupling phases $\Phi_{1,2}^e$ and the resonance mode K_r (linked to the emitter frequency via $2\Delta_e = E_K$) shape GEP dynamics. In the main text, F_K is written as the sum of four vectors

$$F_K = \sum_{\tau,\sigma} \vec{e}_{\tau\sigma}(K), \tag{R13}$$

corresponding to the four decay channels in Fig. 3. Up to a global phase Φ_0, these vectors are:

$$\begin{aligned}
\vec{e}_{ll} &: A_{ll}, \\
\vec{e}_{lr} &: A_{lr}\, e^{i\Phi_2^e} e^{-iKd/2}, \\
\vec{e}_{rl} &: A_{rl}\, e^{i\Phi_1^e} e^{-iKd/2}, \\
\vec{e}_{rr} &: A_{rr}\, e^{i\Phi_1^e} e^{i\Phi_2^e} e^{-iKd},
\end{aligned}$$

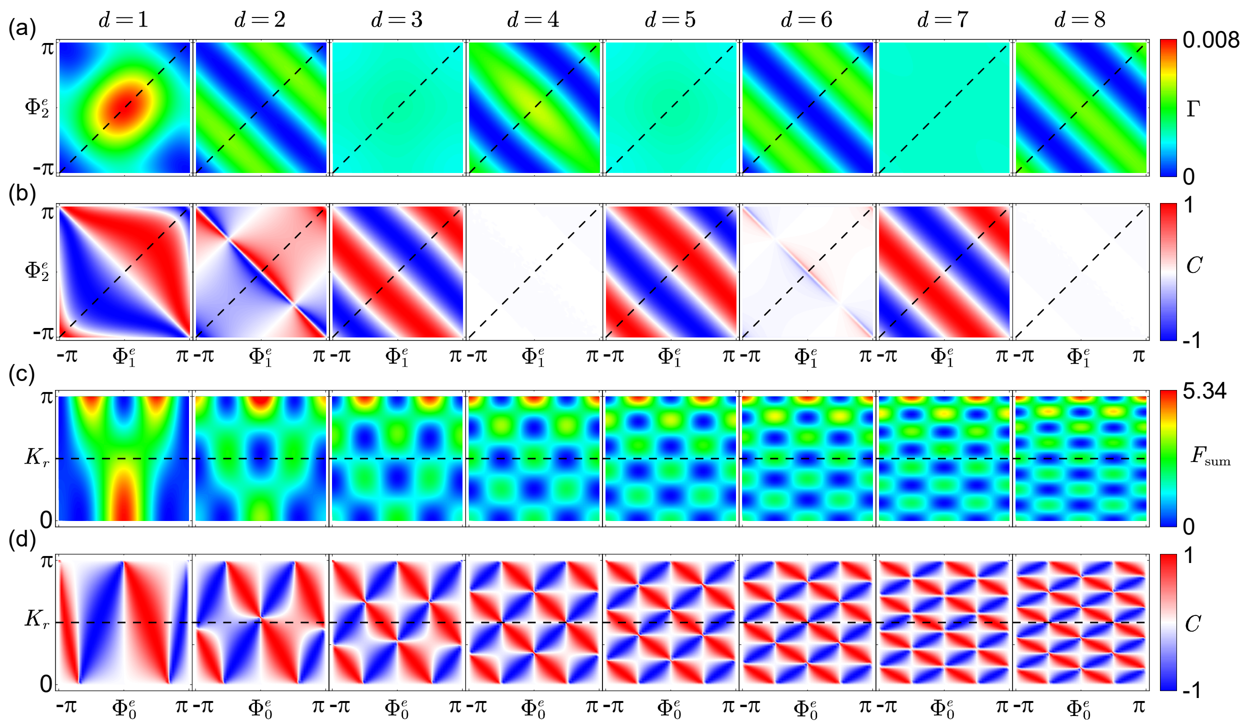

Figure R5. (a) Decay rate and (b) chiral factor, as functions of Φ_1^e and Φ_2^e for different giant-emitter sizes d, with $K_r = \pi/2$ ($\Delta_e = -2.61J$) indicated by the black dashed line in (c, d). (c) $F_{\rm sum} = F(+K_r) + F(-K_r)$ and (d) chiral factor, as functions of K_r and $\Phi_0^e = \Phi_1^e = \Phi_2^e$ [anti-diagonal black dashed line in (a, b)]. The other parameters are the same as in Fig. 2 of the main text.

Owing to symmetry and $D = 0$, the amplitudes satisfy $A_{ll} = A_{rr} = A(0)$ and $A_{lr} = A_{rl} = A(d)$. Equation (S52) then simplified to

$$F(K) = A(0)\left[1 + e^{i\Phi_1^e} e^{i\Phi_2^e} e^{-iKd}\right] + A(d)\left[e^{i\Phi_2^e} + e^{i\Phi_1^e}\right] e^{-iK\frac{d}{2}}. \tag{R14}$$

From this expression, we derive

$$\begin{aligned}
&|F(+K)|^2 + |F(-K)|^2 = \\
&4A(0)^2\left[1 + \cos\left(\Phi_1^e + \Phi_2^e\right)\cos(2\theta)\right] + 8A(0)A(d)\cos(\theta)\left[\cos\left(\Phi_1^e\right) + \cos\left(\Phi_2^e\right)\right] \\
&+ 4A(d)^2[1 + \cos\left(\Phi_1^e - \Phi_2^e\right)],
\end{aligned} \tag{R15}$$

$$\begin{aligned}
&|F(+K)|^2 - |F(-K)|^2 = \\
&8A(0)\sin(\theta)\left\{A(0)\sin(\Phi_1^e + \Phi_2^e)\cos(\theta) + A(d)\left[\sin(\Phi_1^e) + \sin(\Phi_2^e)\right]\right\},
\end{aligned} \tag{R16}$$

where $\theta = Kd/2$.

In Fig. S5(a, b), we plot the decay rate Γ and chiral factor C as functions of Φ_1^e and Φ_2^e for different d, with $K = K_r = \pi/2$ [indicated by black dashed lines in Fig. S5(c, d)]. To isolate interference effects from dispersion-induced group velocity v_g [the denominator of the decay rate in Eq. (S45)], we analyze the sum amplitude $F_{\rm sum} = |F(+K)|^2 + |F(-K)|^2$ and C in the (K, Φ_0^e) plane, setting $\Phi_0^e = \Phi_1^e = \Phi_2^e$ [anti-diagonal in Fig. S5(a, b)]. Via the dispersion relation $2\Delta_e = E_K = -\sqrt{U^2 + 16J^2\cos^2(K/2)}$, the wavevector K directly maps to the emitter frequency.

We identify two distinct regimes:

1. Short separation ($d = 1$). All four channels contribute significantly. Both Γ and C reflect the interference among the four vectors.

2. Long separation [$d > L_u(K_r)$], where $A(d) \simeq 0$. The expressions Eqs. (S54) and (S55) reduce to

$$|F(+K)|^2 + |F(-K)|^2 \approx 4A^2(0)[1 + \cos(\Phi_+^e)\cos(Kd)], \tag{R17}$$
$$|F(+K)|^2 - |F(-K)|^2 \approx 4A^2(0)\sin(\Phi_+^e)\sin(Kd), \tag{R18}$$

   with the symmetric phase $\Phi_+^e = \Phi_1^e + \Phi_2^e$.

   In Fig. S5(a, b) ($K = \pi/2$), Γ and C exhibit pronounced interference patterns:

   - For Γ (panel a): When $\cos(Kd) = 0$ ($d = 3, 5, 7$), Γ becomes uniform. At $d = 4,\ 8$ [$\cos(Kd) = 1$], diagonal striped pattern appear, with alternating bright (green) and dark (blue) bands modulated by $\cos(\Phi_+^e)$; while the pattern inverts for $d = 6$ [$\cos(Kd) = -1$].

   - For C (panel b): When $\sin(Kd) = 0$ ($d = 4,\ 6,\ 8$), C vanishes. At $d = 3,\ 7$ [$\sin(Kd) = -1$], a similar striped pattern appears, with red (positive) and blue (negative) bands separated by nodal lines at $\sin(\Phi_+^e) = 0$ ($\Phi_+^e = 0, \pm\pi$); the contrast flips for $d = 5$ [$\sin(Kd) = 1$].

   In Fig. S5(c, d), the full (K, Φ_0^e) dependence is shown:

   - $F_{\rm sum}$ (panel c) displays a checkerboard-like pattern. Horizontal variations (in Φ_0^e) follow a cosine envelope, while vertical oscillations (in K) become denser with increasing d. The overall intensity grows with K due to the K-dependence of $A(0)$.

   - C (panel d) forms a diamond lattice of alternating red/blue domains, reflecting sine dependence on Φ_0^e and Kd. Similarly, as d increases, vertical oscillation (in K) become denser. Nodal lines (white) are given by $\sin(Kd) = 0$ or $\sin(\Phi_0^e) = 0$.

Moreover, the red (blue) regions in Fig. S5(b, d), corresponding to $C = +1$ ($C = -1$), identify optimal parameters for unidirectional emission: the optimal mode K (i.e., emitter frequency Δ_e) together with coupling phases Φ_1^e and Φ_2^e.

These complex interference results demonstrate that both the super-correlated decay rate Γ and chirality C can be engineered via the geometric parameters d and D, as well as the encoded phases $\Phi_{1,2}^e$, and resonance frequency $2\Delta_e$.

3. Nodal Conditions for the Chiral Factor

The chiral factor C vanishes when the right and left emission intensities balance, i.e., $|F(+K)|^2 - |F(-K)|^2 = 0$. In that scenario, the GEP dynamics recover the small atom behaviour, with non-directional emission [S2]. From Eq. (S55), this occurs when

$$\sin(\theta)\sin\left(\frac{\Phi_1^e+\Phi_2^e}{2}\right)\left[A(0)\cos\theta\cdot\cos\left(\frac{\Phi_1^e+\Phi_2^e}{2}\right)+A(d)\cos\left(\frac{\Phi_1^e-\Phi_2^e}{2}\right)\right]=0. \quad \text{(R19)}$$

This condition is satisfied in three distinct scenarios:

$$\theta = \frac{Kd}{2} = m\pi, \quad m \in \mathbb{Z}, \quad \text{(R20a)}$$

$$\Phi_1^e + \Phi_2^e = 2m\pi, \quad m \in \mathbb{Z}, \quad \text{(R20b)}$$

$$A(0)\cos\theta\cdot\cos\left(\frac{\Phi_1^e+\Phi_2^e}{2}\right)+A(d)\cos\left(\frac{\Phi_1^e-\Phi_2^e}{2}\right)=0. \quad \text{(R20c)}$$

- Equation (S59a), implies that for suitable separations and resonance modes $Kd = 2m\pi$, the system cannot support directional emission regardless of coupling phases, as shown in Fig. S5(b) for $d = 4,\ 6,\ 8$ and the horizontal white bands in Fig. S5(d).

- Equation (S59b), defines a diagonal line in the phase plane, independent of K or d, visible as a white diagonal in Fig. S5(b) and vertical white zones at $2\Phi_0^e = \Phi_1^e + \Phi_2^e = 0, 2\pi$ in Fig. S5(d).

- Equation (S59c), yields curved nodal lines depending on both K, d (via θ) and $A(d)$, accounting for the remaining white features in Fig. S5(b, d).

We hope this explanation, together with the supplementary analysis, resolves the Reviewer's concern.

Reviewer comments

5. Does the optimal Δ_e depend on d (the size of a GE)? If yeas, what is the value of Δ_e in Fig. s4 (which shows the dependence of chirality C on d)? Is it the same for all d's or optimized for each d?

Our reply:

We thank the Reviewer for this insightful question. Indeed, the optimal emitter frequency Δ_e depend on the size d of the GEP.

The optimal condition for chiral emission, corresponding to $|C| \to 1$, is achieved when either $F_{+K_r} = 0$ or $F_{-K_r} = 0$. Through the dispersion relation $2\Delta_e = E_{K_r}$, Δ_e maps directly to the resonant mode K_r. Furthermore, the amplitude F_{K_r} contains an accumulated propagation phase factor $e^{-iK_r x_c^{\tau\sigma}}$ that depends explicitly on both K_r and the spatial separation d between coupling points. Therefore, the interference condition that maximizes chirality and hence the optimal value of Δ_e varies with d.

In the original Fig. S4, we fixed $\Delta_e = -2.61J$ ($K_r = \pi/2$) for all d to illustrate how the decay rate and chirality evolve with increasing emitter size. To fully address the Reviewer's question, we have now added new panels [Fig. S4 (c, d)] in the Supplementary Material, which display C as a function of both the wavevector K (equivalently, Δ_e) and the coupling phase Φ_0^e. These plots explicitly show how the optimal Δ_e shifts with d. A corresponding paragraph has been added on Page [11] to discuss this dependence in detail.

Moreover, the red (blue) regions in Fig. S3(b, d), corresponding to $C = +1$ ($C = -1$), identify optimal parameters for unidirectional emission: the optimal mode K (i.e., emitter frequency Δ_e) together with coupling phases Φ_1^e and Φ_2^e.

For further context regarding Fig. S4(c,d), we refer the Reviewer to our response to the previous comment. We hope this clarification resolves the raised concern.

Reviewer comments

6. In Eq. (19), the decay rates are temporally modulated to optimize state transfer between different sites. Ref. [8] is cited for this. There were earlier works proposing such ideas, see, e.g., PRL 78, 3221 (1997) and PRL 95, 030504 (2005), which may be appropriate references.

Our reply:

We thank the Reviewer for this valuable suggestion and for pointing us to these seminal earlier works. In the revised manuscript, we have added citations to both of these foundational papers alongside Ref. [8] on Page [6].

Reviewer #3

Reviewer comments

In "Nonlinear cascaded quantum network with giant emitters" Wang et al. propose to combine giant emitters with nonlinear waveguides as a way to obtain directional emission of mutiphoton bound states for quantum network applications. As possible applications, they propose the long-distance transfer of an entangled Bell state and or the dissipative generation of multipartite entanglement. They briefly discuss the feasability of an implementation in circuit QED.

Our reply: We thank the Reviewer for giving a comprehensive summary of our work.

Reviewer comments

In my view, the present work builds upon the photon bound-state emission analysis presented in Ref. [49], employing the same approximations and arriving at an almost identical mathematical description of the emission process. The key difference is that, in the current case, the emission can be directional. This arises from the use of giant atoms, which couple to neighboring nodes with different phases—an effect that has been extensively studied in the literature on linear waveguides. The combination of this directionality (introduced by giant atoms) and the same approximations used in the master-equation derivation of Ref. [49] leads to a cascaded master equation involving multiple emitters. The authors identify this equation as equivalent to those previously shown to support remarkable applications in cascaded networks within linear waveguides, such as state transfer and entanglement distribution.

Our reply: We sincerely thank the Reviewer for the thoughtful assessment, which clearly articulates how our work builds upon Ref. [49] by incorporating giant atoms to achieve directional emission, leading to a cascaded master equation and enabling applications such as state transfer and entanglement distribution.

Reviewer comments

Clarity: The combination of these two setups—nonlinear waveguides and giant atoms—requires the reader to grasp two conceptually nontrivial ideas. However, the manuscript devotes only a very limited amount of space to explaining them. As a result, the paper could be made significantly clearer and easier to follow if the authors expanded these sections and provided a more detailed discussion of the underlying concepts.

Our reply: We thank the Reviewer for this valuable suggestion regarding the clarity of our manuscript.

We fully agree that combining nonlinear waveguide QED with the giant-atom configuration involves two conceptually rich frameworks, which may present challenges to readers unfamiliar with either topic. In response to this comment, we have significantly expanded the Introduction (Page [1]) to provide a more accessible overview.

Specifically, the added second paragraph provides a clearer explanation of nonlinear waveguides, emphasizing how on-site photon-photon interactions lead to correlated photon-pair emission. The third paragraph introduces the concept of giant atoms, highlighting how multiple coupling points lead to quantum interference and enable directional emission. These revisions are intended to provide readers with the essential physical intuition to better understand the main results presented in the paper.

Recent progress in engineered quantum platforms has opened promising pathways toward overcoming this challenge, such as superconducting circuit QED via the intrinsic anharmonicity [25-27] or Rydberg atom arrays via dipole blockade [28,29]. A notable example is provided by nonlinear waveguides, which are often modeled by Bose–Hubbard Hamiltonians with on-site photon-photon interactions [30-33]. In such systems, the interplay between nonlinearity and dispersion leads to strongly correlated multiphoton states, where photons can become bound together in real space [34-37]. These correlated states, in turn, can mediate supercorrelated radiation dynamics and enable the generation of correlated photon pairs [38-42].

In parallel, the emerging paradigm of giant atoms has attracted considerable attention [43-47]. A giant atom couples to a photonic or phononic bath at multiple discrete points, with an effective size comparable to the operating wavelength [48-54]. This multi-point coupling structure gives rise to multiple decay channels that interfere quantum mechanically. By engineering the geometry and phase of these coupling points, one can tailor the interference to facilitate novel phenomena such as decoherence-free dipole-dipole interactions [55-58], oscillating bound states [59-62], and chiral quantum effects [63-65].

We hope these enhancements make the manuscript clearer and easier to follow.

Reviewer comments

Novelty and relevance: I find the idea of combining giant atoms with nonlinear waveguides novel and potentially interesting. However, its relevance to the field of quantum networks is not at all clear. To the best of my knowledge, directional emission of correlated photons can already be achieved using linear waveguides. For example, this can be realized with two directly interacting emitters, or with a single emitter possessing multiple energy levels or enabling two-photon transitions. It would therefore be important for the authors to clarify what specific advantages from introducing nonlinear waveguides, as opposed to the well-studied linear systems that already support cascaded quantum networks.

Our reply: We sincerely thank the Reviewer for this insightful comment and for recognizing the novelty of combining giant atoms with nonlinear waveguides. We appreciate the opportunity to further clarify the specific advantages and relevance of our approach compared to well-studied linear-waveguide schemes.

We have extensively revised the manuscript to address this point. The key additions and adjustments are summarized as follows.

1. **Clarifying the limitations of linear cascaded networks and our advance.**

   As the Reviewer rightly notes, directional emission of single photons or correlated photons can indeed be achieved in linear systems. However, those in linear system and our proposal are distinct in physical mechanism: conventional protocols employ single photons as information carriers, whereas our approach exploits doublons (two-photon bound states) to enable **joint two-excitation transfer**. This key difference allows our setup to transfer two-photon (two-qubit) quantum states between remote network nodes in **a single-step operation**, in contrast to standard methods, which are limited to transferring one excitation (one qubit) at a time.

   This capability is particularly advantageous for distributing multi-emitter entangled states. For example, in existing protocols, such as *Deterministic multi-qubit entanglement in a quantum network* [Fig. 3, adopted from Nature 590, 571 (2021)] **transferring a 3-qubit GHZ state requires three sequential single-qubit transfer operations, together with plenty of local gate operations.** By contrast, our architecture, where

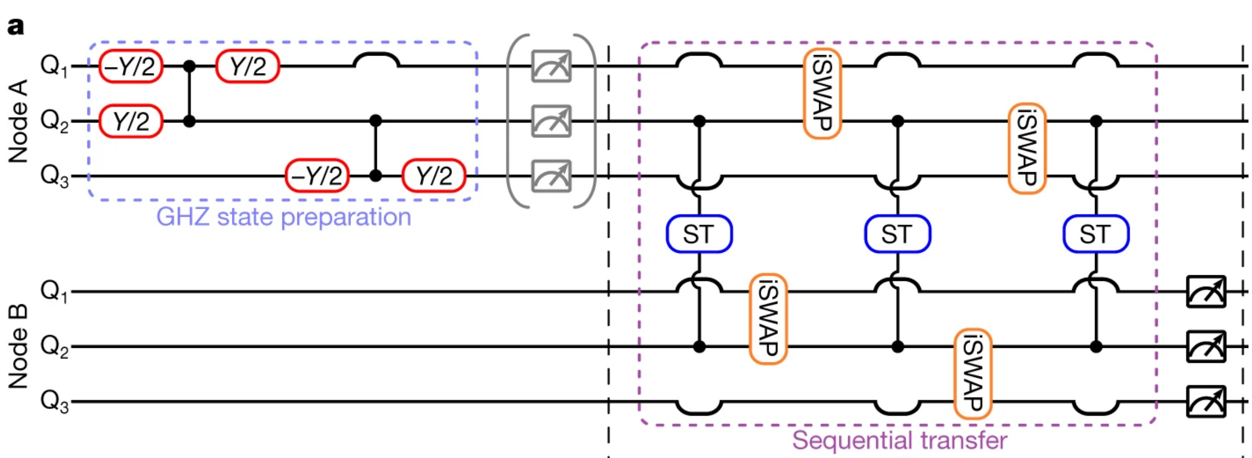

Figure R6. Schematic of the GHZ state preparation and the sequential state-transfer (ST) protocol in *Deterministic multi-qubit entanglement in a quantum network*. The figure is taken from *Nature 590, 571 (2021)*.

   two emitters per node collectively couples to a nonlinear waveguide, enables the **direct and simultaneous transfer of two correlated excitations**. Thus, a two-qubit entangled state prepared at node A, such as

$$|\Psi_{\mathrm{A}}(t_0)\rangle = c_e^{\mathrm{A}}|e,e\rangle + c_g^{\mathrm{A}}|g,g\rangle,$$

can be mapped onto node B in a single step, preserving entanglement without intermediate operations.

To clearly frame this distinction, we have first added an introduction of generating directional single-photon research in the revised manuscript on Page [5].

Contrasting linear setups, such as interacting emitter pairs [6,7], multiple-level atoms [69], and superradiance of atom ensembles (time-Dicke states) [70], our proposal utilizes supercorrelated photons as “flying qubits", enhancing numerous many-body applications.

We have also clarified this distinction on Page [6] of the revised manuscript by adding *Nature 590, 571 (2021)* as Ref [71]:

Unlike conventional multipartite entanglement transfer with single flying qubits [71], this nonlinear interface enables entanglement state transfer in a single-step operation. For example, an initial entangled state of GEP A, $|\Psi_{\mathrm{A}}(t_0)\rangle = c_e^{\mathrm{A}}|e,e\rangle + c_g^{\mathrm{A}}|g,g\rangle$, can be directly mapped onto GEP B as $|\Psi_{\mathrm{B}}(t_0)\rangle = c_e^{\mathrm{B}}|e,e\rangle + c_g^{\mathrm{B}}|g,g\rangle$ without sequential operations.

2. **Highlighting the broader implications for network architecture.**

   To better connect our work with quantum network, we have restructured the end of Section “Nonlinear Cascaded Quantum Network” to emphasize the nonlinear cascaded master equation. In particular, we have also added a concluding summary on Page [7]

   Following the methods in Fig. [4], our proposal enable single-step transfer of an arbitrary $\mathcal{N}$-qubit GHZ state, $|\psi_0\rangle = c_e|e\rangle^{\otimes\mathcal{N}} + c_g|g\rangle^{\otimes\mathcal{N}}$, between two $\mathcal{N}$-body nodes, without decomposing it into sequential single-excitation processes. In summary, our work demonstrates that nonlinear waveguides can be configured as multiphoton buses supporting advanced many-body quantum applications in future study.

Our work thus establishes nonlinear waveguides as a promising platform for quantum buses, unlocking potential applications inaccessible to linear waveguides. We hope the revised manuscript now more clearly highlights the distinctness of our proposed nonlinear cascaded quantum network. We thank the Reviewer again for prompting the comparison with prior literature in linear waveguide, which has also helped us better recognize and present the advantages of our approach.

Reviewer comments

Leaving aside this major point, I have a few additional comments and questions:

Our reply: We thank the Reviewer for these insightful comments. We have carefully considered each suggestion and have revised the manuscript accordingly. Our point-by-point responses are provided below.

Reviewer comments

-Can the choice of phases be adjusted to recover the non-directional emission discussed in Ref. [49]? Addressing this point (for example, in page 4 when directional emission is introduced) would help strengthen the conceptual link between the present results and those of Ref. [49].

Our reply:

We thank the Reviewer for this valuable suggestion, which helps to clarify the connection between our work and Ref. [49]. Indeed, in our proposal, when the chiral factor vanishes, i.e.,

$$|F(+K)|^2 - |F(-K)|^2 = 0,$$

the emission behavior of the CEP recovers that of a small atom, exhibiting the non-directional emission characteristic of Ref. [49].

To clearly identify the parameter regimes leading to this condition, we have added a new subsection (Section II.C.3 *"Nodal Conditions for the Chiral Factor"*) in the Supplementary Material on Page [11], which provides an analytical derivation of the requirement for $C = 0$

3. Nodal Conditions for the Chiral Factor

The chiral factor C vanishes when the right and left emission intensities balance, i.e., $|F(+K)|^2 - |F(-K)|^2 = 0$. In that scenario, the GEP dynamics recover the small atom behaviour, with non-directional emission [S2]. From Eq. (S55), this occurs when

$$\sin(\theta)\sin\left(\frac{\Phi_1^e+\Phi_2^e}{2}\right)\left[A(0)\cos\theta\cdot\cos\left(\frac{\Phi_1^e+\Phi_2^e}{2}\right)+A(d)\cos\left(\frac{\Phi_1^e-\Phi_2^e}{2}\right)\right]=0. \quad \text{(R21)}$$

This condition is satisfied in three distinct scenarios:

$$\theta = \frac{Kd}{2} = m\pi, \quad m \in \mathbb{Z}, \quad \text{(R22a)}$$

$$\Phi_1^e + \Phi_2^e = 2m\pi, \quad m \in \mathbb{Z}, \quad \text{(R22b)}$$

$$A(0)\cos\theta\cdot\cos\left(\frac{\Phi_1^e+\Phi_2^e}{2}\right)+A(d)\cos\left(\frac{\Phi_1^e-\Phi_2^e}{2}\right)=0. \quad \text{(R22c)}$$

- Equation (S59a), implies that for suitable separations and resonance modes $Kd = 2m\pi$, the system cannot support directional emission regardless of coupling phases, as shown in Fig. S5(b) for $d = 4,\ 6,\ 8$ and the horizontal white bands in Fig. S5(d).

- Equation (S59b), defines a diagonal line in the phase plane, independent of K or d, visible as a white diagonal in Fig. S5(b) and vertical white zones at $2\Phi_0^e = \Phi_1^e + \Phi_2^e = 0, 2\pi$ in Fig. S5(d).

- Equation (S59c), yields curved nodal lines depending on both $K,\ d$ (via θ) and $A(d)$, accounting for the remaining white features in Fig. S5(b, d).

Furthermore, in the main text on Page [5], we have incorporated a discussion following the introduction of directional emission, explicitly linking our results to the non-directional case discussed in Ref. [49].

In the white region where $C = 0$, the GEP dynamics recover the small-atom behaviour with non-directional emission [38]. The specific parameter regimes corresponding to $C = 0$ are discussed in Section II C of Supplementary Material.

We believe these additions effectively strengthen the conceptual connection between the two works and thank the Reviewer again for the valuable suggestion.

Reviewer comments

-What is the main source of imperfection that limits the reported fidelity to 98%, rather than 100%?

Our reply: We thank the Reviewer for this insightful question regarding the origin of the fidelity limitation in our state transfer protocol.

The achieved fidelity of approximately 98% (as opposed to 100%) is primarily limited by the following physical and practical factors:

- **Intermediate single-photon process:** Prior to supercorrelated radiation, the dynamics involve population of intermediate single-photon states, as shown by the shadowed curves in Fig. 2(a). The non-ideal spontaneous emission characteristics during this intermediate stage slightly perturb the ideal evolution required for perfect state transfer.

- **Finite time window:** Theoretically, perfect state transfer requires modulation pulses extending from $t \to -\infty$ to $t \to +\infty$. In our numerical simulation, however, we necessarily employ a finite time window, which introduces minor deviations from the perfect fidelity.

To address this point, we have added the following clarification in the revised manuscript on Page [6]:

At the final time t_f, one finds that $\{|c_e^{\mathrm{A}}(t_f)|^2, \sum_K |c_K(t_f)|^2\} \simeq 0$, and the absorption efficiency is $|c_e^{\mathrm{B}}(t_f)|^2 \simeq 98\,\%$. This value is primarily limited by the finite simulation time window and the non-ideal spontaneous emission dynamics during the single-photon intermediate process.

We hope this explanation addresses the Reviewer's question.

Reviewer comments

-The use of the term "intriguing" in this context does not seem appropriate for a scientific manuscript, in my opinion. A more precise and descriptive characterization of the result would be preferible.

Our reply: We thank the Reviewer for the valuable suggestion regarding the use of subjective language. In response, we have removed the term "intriguing" throughout the manuscript and replaced it with more precise and objective phrasing. The two specific instances have been revised as follows:

- We now demonstrate a high-fidelity process for entangled-state transfer...
- We further consider an application in which the three GEs in two remote nodes are pumped via three-photon parametric down-conversion processes...

Reviewer comments

-The paragraph on experimental feasibility appears to closely follow that of Ref. [49], suggesting that an independent evaluation may not have been performed. It would be useful if the authors could comment on the coupling strengths (g values) reported in the cited giant-atom experiments and discuss whether these are consistent with the parameters used in their simulations.

Our reply:

We thank the Reviewer for this important point regarding experimental feasibility and for prompting a more independent evaluation. In response, we have thoroughly revised the corresponding section on Page [7] to provide a dedicated evaluation of the experimental parameters relevant to giant atoms.

Our proposal is feasible in circuit-QED systems [27,75,76]. An array of coupled transmon qubits [25] can be configured as the nonlinear waveguide. The hopping rate and Kerr nonlinearity of such an array demonstrated in experiments [30,77-79] are on the order of $J/2\pi \sim 50\,\mathrm{MHz}$ and $U/2\pi \sim 200\,\mathrm{MHz}$, respectively.

The giant-atom configuration, with multiple discrete coupling points to a waveguide, has already been experimentally realized in Refs [52,56]. In our scheme, the relative coupling phases required for directional emission can be dynamically tuned via parametric modulation [65]. The transmon anharmonicity $U_{\mathrm{giant}}/2\pi \sim 300\,\mathrm{MHz}$ supports the two-level approximation for the emitters. Furthermore, time-dependent interactions between superconducting giant atoms and the nonlinear waveguide can be realized using methods from Ref. [65,80], achieving a coupling strength of $g/2\pi = 0.1J/2\pi \sim 5\,\mathrm{MHz}$.

Under these parameters, the supercorrelated emission rate is estimated as $\Gamma_{\pm}/2\pi \sim 1\,\mathrm{MHz}$ (see Supplementary Materials), which is much larger than the intrinsic decoherence rate of a circuit-QED platform [81,82]. Therefore, the phenomena predicted in this work are possible to observe in current circuit-QED setups.

CONCLUSION

In conclusion, we really thank the Reviewers for very useful comments and constructive criticism. Those comments help us improve the paper significantly. We have addressed all comments in the revised manuscript and highlighted the changes there. We hope the Reviewers now find our paper ready for publication in Communications Physics.

Yours sincerely,

the authors

RESPONSE LETTER TO REVIEWERS

Reviewer #1

Reviewer comments

- Entanglement transfer with linear waveguides -

To my comment on the novelty and relevance, the authors respond that "conventional methods are limited to transfer one excitation at a time". However, they also say "As the Reviewer rightly notes, directional emission of single photons or correlated (I assume multiphoton?) photons can indeed be achieved in linear systems". These two statements appear internally inconsistent and require clarification.

If the authors believe that nonlinear waveguides provide an "alternative" route for entanglement state transfer in a single-step operation, then they should explicitly acknowledge and cite existing approaches based on linear waveguides that achieve comparable functionality, and clearly position their method as an alternative within this broader landscape. Conversely, if the authors claim that nonlinear waveguides constitute the only known approach (to the best of current knowledge) enabling entanglement state transfer in a single-step operation, this claim should be stated explicitly.

At present, the manuscript remains too vague on this point. For instance, the authors write: "Unlike conventional multipartite entanglement transfer with single flying qubits, this nonlinear interface enables entanglement state transfer in a single-step operation"

-Do linear waveguides support emission of two-photon states? If yes, then it seems that entanglement-transfer is also possible using linear waveguides. For example Ref.[69] suggests that multi-photon emission is possible with linear waveguides.

Our reply: We thank the Reviewer for this insightful comment. In a quantum network, both the "flying qubits" and the structure of each quantum node determine the class of quantum information protocols that can be implemented.

We agree that linear waveguide QED setups, such as the multiphoton emission scheme in Ref. [69], can generate correlated photon pairs from a single multi-level emitter. However, in such approaches, the multi-level atom is effectively described as a single effective two-energy-level qubit via adiabatic elimination of the intermediate state. Consequently, the quantum node does not host genuine multipartite entanglement among multiple stationary qubits, and cannot support protocols requiring pre-engineered many-body states (e.g., GHZ states) to be transferred between remote nodes.

In contrast, our scheme operates in the multi-excitation manifold of multiple stationary qubits and enables the transfer of genuine GHZ-type entanglement, as detailed in the following response regarding the advantages over linear-waveguide approaches.

To clarify this point, we have added the following paragraph from Pages 6 to 7:

In linear waveguide QED setups, a single multi-level emitter can be adiabatically reduced to a single effective qubit for correlated-photon emission [69]. Since such a node lacks internal multipartite structure, it cannot support the **direct** transfer of many-body entangled states (e.g., GHZ states) between distant nodes.

Reviewer comments

-Also, it is not at all clear to me that single photons cannot be used for entanglement transfer. In quantum memories based on atomic ensembles, doesn't a single photon generate a multipartite entangled state in the atoms?

Our reply: We thank the Reviewer for this important point. It is true that a single photon can generate multipartite entanglement in atomic ensembles, for example, a **single-excitation W state** via collective absorption. However, such states belong to a different entanglement class than the **GHZ-type states** considered in our work. Crucially, W and GHZ states cannot be interconverted via local operations and classical communication (LOCC), and they exhibit fundamentally distinct properties (e.g., robustness to particle loss vs. maximal nonlocality). As the reply to the next comment, our scheme enables **deterministic transfer** of GHZ-type entanglement without any local operation.

Reviewer comments

Similarly, the statement "Contrasting linear setups,..., our proposal utilizes supercorrelated photons as "flying qubits", enhancing numerous many-body applications" is too vague. The manuscript should explicitly identify which many-body applications are enhanced and explain how the use of supercorrelated photons provides a concrete advantage over linear-waveguide-based approaches.

Our reply: As we wrote in previous reply, existing protocols, such as GHZ-state entanglement transfer in a linear quantum network [Fig. R1, adopted from Nature 590, 571 (2021)], requires sequential single-qubit transfer operations, together with plenty of local gate operations. To the best of our knowledge, our architecture is the first to enable **deterministic, single-step transfer of a pre-engineered GHZ state between multi-emitter nodes using correlated flying photonic states**.

Therefore, we thank the Reviewer for helping us find the suitable position of our research within the existing literature. Accordingly, we have revised the manuscript on Page 7 as

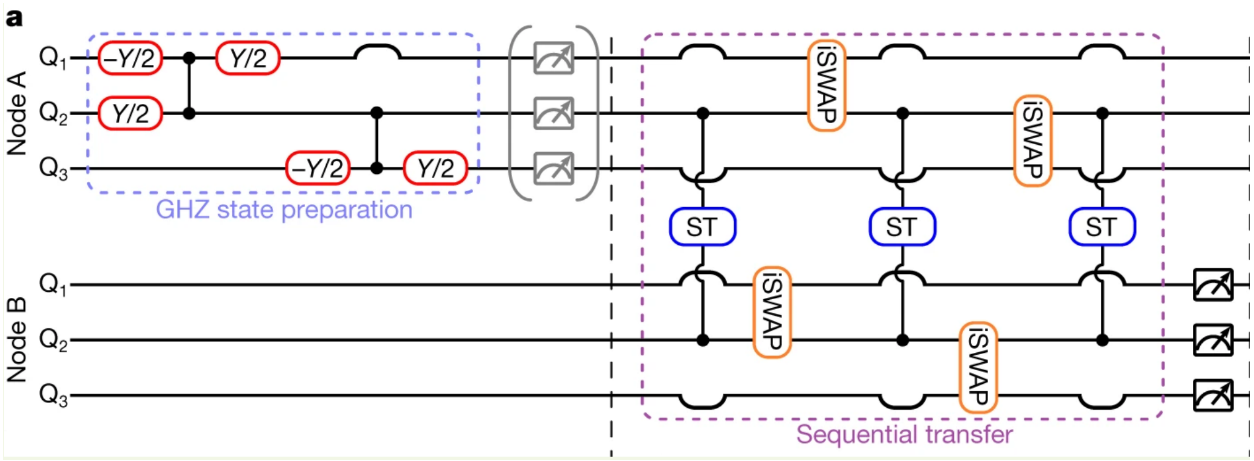

Figure R1. Schematic of the GHZ state preparation and sequential state-transfer (ST) protocol in deterministic multi-qubit entanglement distribution. The figure is reproduced from Nature **590**, 571 (2021) for peer-review purposes only.

follows:

Unlike conventional GHZ-state distribution in linear waveguides [71], which requires sequential single-photon transmissions and numerous local operations, our nonlinear cascaded interface accomplishes this many-body task without the need for sequential control or post-processing. For example, an initial entangled state of GEP A, $|\Psi_{\rm A}(t_0)\rangle = c_e^{\rm A}|e,e\rangle + c_g^{\rm A}|g,g\rangle$, can be directly mapped onto GEP B as $|\Psi_{\rm B}(t_0)\rangle = c_e^{\rm B}|e,e\rangle + c_g^{\rm B}|g,g\rangle$ in a single-step operation.

Reviewer comments

- 98% fidelity -

In response to my question regarding the dominant sources of imperfection, the authors state that the error arises from (1) finite transfer time and (2) intermediate single-photon processes.

The authors should quantify the relative contributions of these two mechanisms to the reported 2% infidelity. In my understanding, the error associated with (1) can reduced by increasing the transfer time. In contrast, the imperfection arising from (2) seems more fundamental, as it is intrinsic to the dynamics and may require modification of system parameters or operating regimes to mitigate.

The manuscript would benefit from a discussion addressing how each error contribution can be reduced. For example, are there parameter regimes in which these intermediate single-photon processes are further suppressed ? Clarifying whether this source of imperfection sets

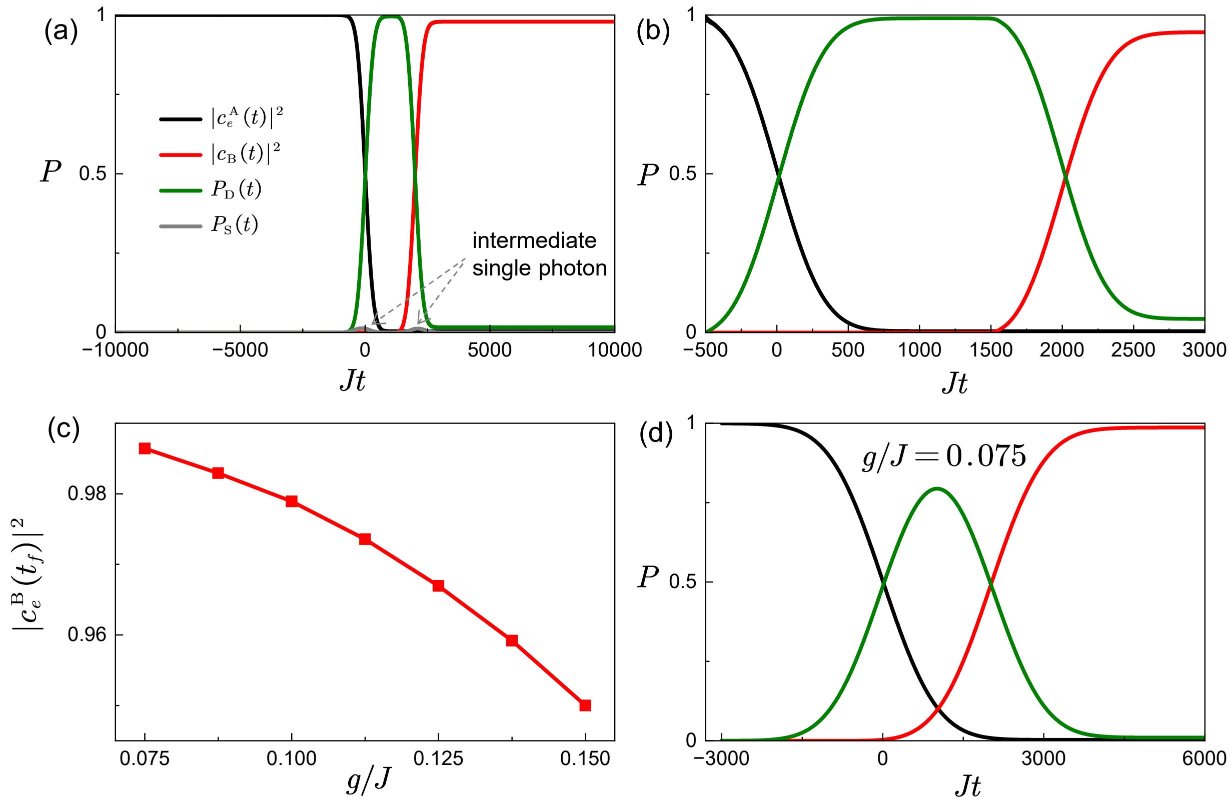

Figure R2. (a,b) State-transfer process under a longer ($t \in [-10000, 10000]$) and a shorter ($t \in [-500, 3000]$) time window compared to the main text ($t \in [-1500, 3000]$), with coupling $g/J = 0.1$. The gray curve indicates intermediate single-photon population $P_S(t) = \sum_{m,k} |c_{mk}(t)|^2$. (c) Fidelity as a function of g/J. (d) State-transfer process for a weaker coupling $g/J = 0.075$. Other parameters are the same as in Fig. 4 of the main text.

a fundamental limit, or whether it can be engineered away, is essential for assessing the scalability and practical relevance of the proposal.

Our reply:

We thank the Reviewer for prompting us to clarify the sources of infidelity.

The error from source (1) can be suppressed by adopting a longer time-window. In Fig. R2(a), we take a sufficiently long time-window, $t \in [-10000, 10000]$, to suppress the infidelity from (1) as much as possible. The resulting fidelity of is only slightly higher ($\sim 0.1\%$) than the reported in the main text, confirming that the time window used ($t \in [-1500, 3000]$) is already long enough for the transfer process. Therefore, nearly all the 2% infidelity reported in the main text (Fig. 4) stems from the intermediate single-photon states. In contrast, for a shorter time window $t \in [-500, 3000]$ in Fig. R2(b), the fidelity decreases to 95%. Further discussion of this imperfection mechanism can be found in Phys. Rev. B **84**, 014510 (2011) and Phys. Rev. A **84**, 042341 (2011).

We now discuss source (2). In our analytical derivations, we assume that Δ_e is strongly detuned from the single-photon scattering states, which strongly suppresses the single-photon probability amplitudes. This enables us to adiabatically eliminate c_{mk} by assuming $\dot{c}_{mk}(t) = 0$, i.e.,

$$c_{mk}(t) \simeq -\left[\sum_{\tau=l,r} \frac{g}{\delta_k\sqrt{N}} e^{-ikn^{\tau}_{m'}} e^{i\phi^{\tau}_{m'}} c_e(t) + \sum_{K} \frac{g}{\delta_k} e^{-i\phi^{\tau}_{m}} M(k, n^{\tau}_{m}, K) c_K(t)\right]. \tag{R1}$$

In the ideal limit, $c_{mk}(t) = 0$. However, in practice [gray curves in Fig. R2(a)], $c_{mk}(t)$ is not identically zero. Such far-detuned emitter dynamics has been extensively studied, for example, in Phys. Rev. A 93, 033833 (2016), Phys. Rev. A 96, 043811 (2017) and related works. These intermediate single-photon states affect doublon emission and consequently the overall state-transfer fidelity.

From Eq. (R1), reducing the coupling strength g can suppress the intermediate single-photon states amplitudes and thus the error from (2). Fig. R2(c) shows that the fidelity increases as g decreases. However, the decay rate of the emitter [Eq. (16) in the main text] is given by

$$c_e(t) = \exp\left(-\frac{\Gamma_+ + \Gamma_-}{2} t\right), \quad \Gamma_\pm = \frac{g^4}{v_g J^2} \left|F_{\pm K_r}\right|^2, \tag{R2}$$

which scales as g^4. Therefore, reducing g significantly lengthens the required state-transfer time-window, as shown in Fig. R2(d) for $g/J = 0.075$, where $t \in [-3000, 6000]$ is twice as long as for $g/J = 0.1$. Thus, while intermediate single-photon contributions can be suppressed through parameter engineering, their complete elimination would require infinitely long transfer times—an unphysical condition in any real experiment.

In conclusion, suppressing both sources of infidelity, the intermediate single-photon states and the finite transfer time, requires increasing the transfer duration. However, a longer transfer time not only slows down the quantum information protocol but also allows other decoherence channels to become significant. Therefore, this trade-off leads to an optimal transfer time for realistic experimental implementations.

To clarify this point, we have revised the discussions on Page 6 as follows:

This value is primarily limited by the intermediate single-photon process and the finite transfer time [9]. Reducing the coupling strength during state transfer suppresses the intermediate single-photon amplitudes, thereby improving the corresponding fidelity. However, it also reduces the doublon emission rate, leading to a longer transfer time. This not only slows down the quantum information protocol but also enhances the impact of other decoherence channels. Consequently, in a realistic experimental implementation, an optimal coupling strength $g(t)$ might be chosen to balance transfer fidelity with operation speed.

We thank the Reviewer again for this helpful comment, which has allowed us to present the infidelity analysis more clearly.

Reviewer comments

Also, I do not understand the use of the term "simulation" in "finite simulation time window". I understand the authors refer an error due to finite transfer time. This will also appear in real setups and does not have to do with specifics of the numerical simulation.

Our reply:

We thank the Reviewer for this comment regarding the terminology. To accurately reflect the physical nature of this error source, we have revised the manuscript accordingly, replacing “finite simulation time window” with “finite operation time” or “finite transfer time” throughout the text.

Reviewer comments

— The dark state condition — "Because dark-state conditions always hold in this nonlinear cascaded system, the correlated-two-photon field is trapped between the two GEPs without leaking outside" In the context of quantum-state transfer, modulation of the light-matter coupling is needed in order to satisfy a "dark state condition" and thus achieve perfect transfer. To state that "dark-state conditions always hold in this nonlinear cascaded system" is confusing since it suggests modulation is not needed to achieve perfect transfer.

Our reply:

We thank the Reviewer for this clarification. We agree that the dark-state condition relies on the engineered time-dependent decay rates specified in Eq. (20). The original wording was misleading, and we have revised it accordingly. We revised the sentence on Page 6

Given that the decay rates are modulated according to Eq. (20), the dark-state conditions hold in this nonlinear cascaded system, and the correlated-two-photon field is trapped between the two GEPs without leaking outside.

CONCLUSION

We thank the Reviewer again for his/her careful reading of our manuscript, and for the useful comments and constructive criticism. We have addressed all the comments in the revised manuscript and highlighted the changes there. We hope the Reviewer now finds our paper ready for publication in Communications Physics.

Yours sincerely,

the authors

RESPONSE LETTER TO REVIEWERS

Reviewer #1

Reviewer comments

The work by Wang et al (number COMMSPHYS-25-1042-T) studies the problem of two-legged giant atoms weakly- coupled to a non-linear homogeneous coupled cavity array, in which a boundphoton minibands exist regardless of the sign of the interaction. For instance, in case of two giant atoms (so called "giant emitter pair" GEP), both resonant to the mini-band, the authors discuss a mechanism for chiral emission of bound photon pairs, which is resilient to different geometric configurations of the giants, phase differences in the coupling etc. Building on that, together with technique of optimal control in time of the coupling strengths, the authors propose a so-called non-linear cascaded network, in which excitations can be deterministically transferred between different GEPs, or entanglement can be efficiently created between remote GEPs. In the end, the authors argue that this mechanism can be extended to configurations in which more than two photons are involved and discuss potential implementations within the paradigm of circuit-QED.

Our reply: We thank the Reviewer for giving a comprehensive summary of our work.

Reviewer comments

While the idea is potentially interesting, bridging non-linear systems with waveguide-QED, I cannot recommend it for publication before the authors have addressed the following points.

Our reply: Thank the Reviewer for recognizing the potential interest of our work. We appreciate the opportunity to address the concerns raised and have carefully revised the manuscript accordingly. Below, we provide a point-by-point response to the reviewer's comments.

Reviewer comments

1. When introducing the model of a non-linear coupled cavity array, the authors discuss and derive the dispersion law of the miniband of bound photons, see Eq. 5. This result though only holds when U<0 (attractive interaction), as correctly stated in the supplementary material. In general, since the sign of the interaction seems not to be so important for the discussed phenomenology, I would amend this part by including both solutions (or else justify why they need U<0 for everything to work).

Our reply: We sincerely thank the Reviewer for this insightful comment.

The wavefunction under repulsive interaction ($U > 0$) exhibits a notable sign alternation at nearest-neighbor r, which in turn influences the emitter's dynamics.

In response, we have added the following sentence in the main text (Page [2]) to clarify the main focus of our study:

Throughout this work, we focus on systems with attractive interactions $U < 0$. A detailed discussion of the repulsive case $U > 0$ is provided in Section I and II D of Supplementary Material.

Additionally, we have expanded the Supplementary Material to include further discussion on the repulsive case ($U > 0$):

1. In Sec. S I, we now provide the wavefunction for $U > 0$ and include a figure to visually compare the energy structure and wavefunctions for both $U > 0$ and $U < 0$.

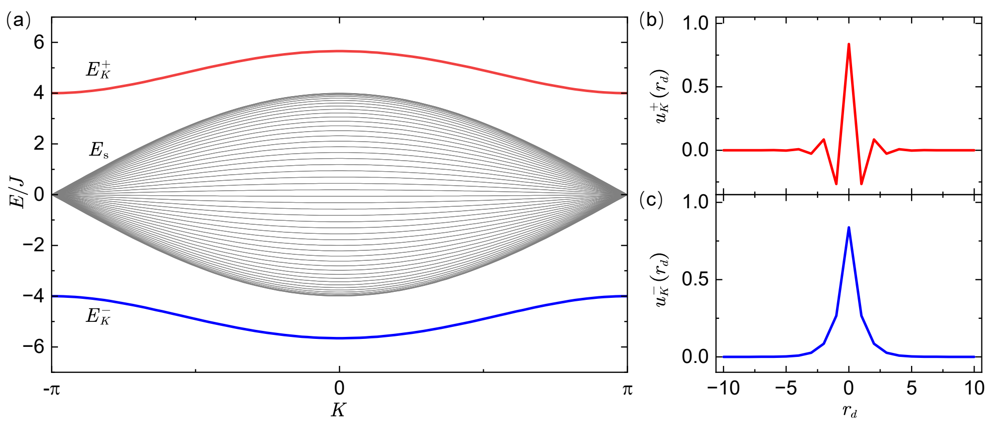

Figure R1. (a) Spectrum of the two-photon subspace. The bound states $E_K^{\pm}$ are given by Eqs. (S14) and (S15); while the scatter state is given by Eq. (S20). (b, c) Wavefunctions $u^{\pm}K(r_d)$ of the bound states at $K = \pi/2$, given by Eqs. (S16) and (S17). The superscript $\pm$ denotes the sign of the interaction U.

The wave function for mode K is written as

$$u_K(r_d) = \frac{G_K^0(E, r_d = 0)U}{1 - G_K^0(E, r_d = 0)U} G_K^0(E, r_d)$$
$$= \frac{G_K^0(E, r_d = 0)U}{1 - G_K^0(E, r_d = 0)U} \frac{1}{2\pi} \int dq \, \frac{e^{iqr_d}}{E + 4J\cos(\frac{K}{2})\cos q}.$$

Then, the wavefunction is written as [S1-S3]

$$U > 0, \quad u_K(r_d) = u_0(-1)^{|r_d|} \exp\left[-\frac{|r_d|}{L_u(K)}\right], \tag{R1}$$

$$U < 0, \quad u_K(r_d) = u_0 \exp\left[-\frac{|r_d|}{L_u(K)}\right], \tag{R2}$$

where u_0 is a normalization factor and the decay length for two-photon correlations in space is

$$L_u(K) = -\left[\ln\left(\frac{\sqrt{U^2+16J_K^2}-|U|}{4J_K}\right)\right]^{-1}, \tag{R3}$$

with $J_K = J\cos(K/2)$. Note that $L_u(K)$ rapidly decreases when increasing the nonlinear parameter U. Eventually, the wave function of the doublon state is written as

$$\Psi_{\mathrm{d}} = \frac{1}{\sqrt{2}}\sum_{m,n} e^{iK\frac{m+n}{2}} u_K(m-n). \tag{R4}$$

In Fig. S1, we plot the band structure $E_K^{\pm}$ versus K and the wavefunction $u_K^{\pm}(r_d)$ versus r_d at $K = \pi/2$. The superscript $\pm$ corresponds to the sign of the interaction U. The scattering state is plotted for reference [S3]

$$E_{\mathrm{s}} = -4J\cos(K/2)\cos(q), \tag{R5}$$

with relative momentum q.

We focus on the case $U < 0$ throughout the article and a discussion of how $U > 0$ affects these conclusions follows in the Sec. S II D.

2. We have added a new subsection titled "**D. Results for repulsive interaction** $U > 0$" to systematically discuss the effects of repulsive interactions $U > 0$.

D. Results for repulsive interaction $U > 0$

We now turn to the case of repulsive interaction $U > 0$. By replacing the dispersion relation and the wavefunction in Eqs. (15) and (17) with those in Eqs. (16) and (18) throughout the derivation, we obtain the numerical and analytical results for $U > 0$. Figure. S6 displays the decay rate Γ and the chiral factor C as functions of the phase $\Phi_{1,2}^e$ over an extended range of $[-2\pi, 2\pi]$, comparing repulsive ($U > 0$) and attractive ($U < 0$) interactions. Under a π-phase shift, the decay rate remains invariant, while the chirality is reversed due to the energy relation $E_K^{(U>0)} = -E_K^{(U<0)}$. To illustrate these dynamics, we present the time evolution and the photonic field distribution for two cases: (i) $U < 0$, $\Delta_e < 0$, $\Phi_{1,2}^e = -\pi/5$ and (ii) $U > 0$, $\Delta_e > 0$, $\Phi_{1,2}^e = -\pi/5 + \pi = 4\pi/5$. These distinctive properties stem from the sign alternation of the wavefunction between nearest-neighbor r under repulsive ($U > 0$), combined with the reversal of the dispersion relation, as shown in Fig. S1.

We hope these revisions adequately address the Reviewer's valuable point and improve the clarity and completeness of the manuscript.

Reviewer comments

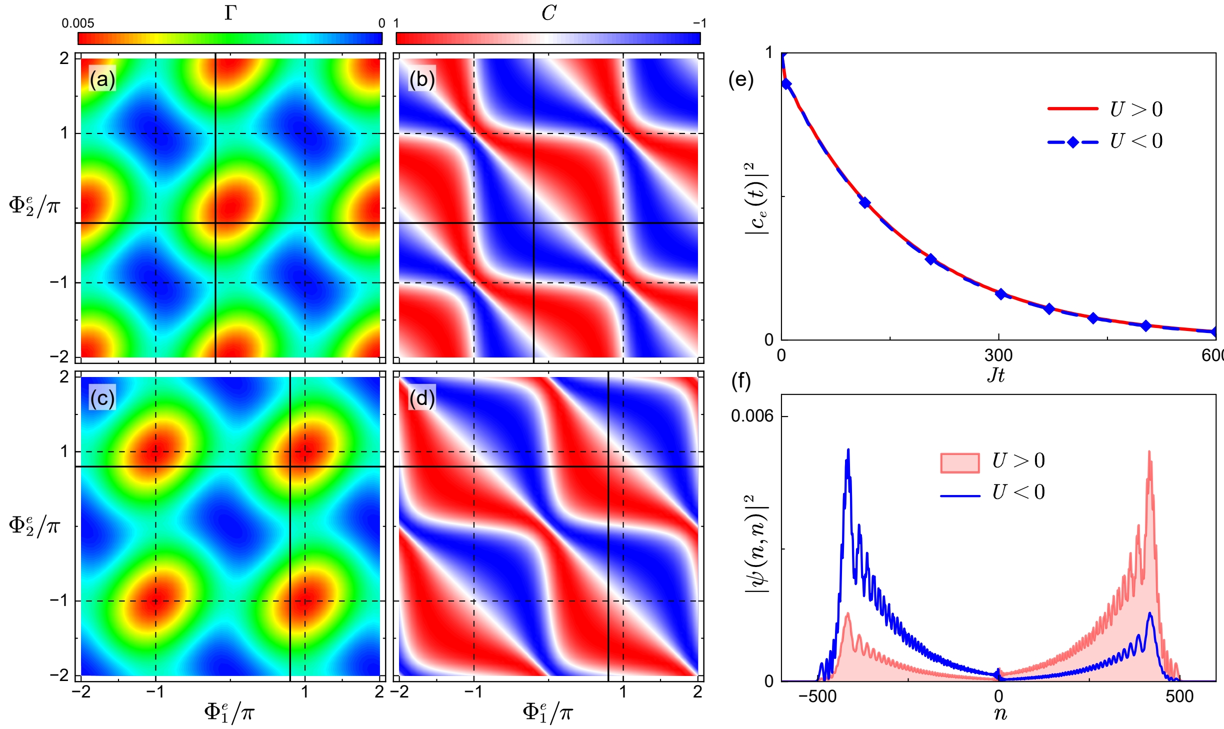

Figure R2. (a) Decay rate Γ and (b) chiral factor C as functions of $\Phi_1^(e)$ and $\Phi_2^(e)$ over $[-2\pi, 2\pi]$ for the attractive interaction $U < 0$. (c, d) Corresponding plots of Γ and C for the repulsive interaction $U > 0$. Dashed lines mark the first Brillouin zone boundaries. Solid lines indicate the parameter sets $\Phi_1^e, \Phi_2^e = -\pi/5$ (for $U < 0$) and $4\pi/5$ (for $U > 0$) used in (e) and (f). (e) Time evolution of $|c_e(t)|^2$. (f) Photonic field distribution $|\psi(n,n)|$ at $Jt = 600$. In (e) and (f), red curves correspond to $U > 0$, $\Delta_e > 0$, and $\Phi_{1,2}^e = 4\pi/5$; blue curves correspond to $U < 0$, $\Delta_e < 0$, and $\Phi_{1,2}^e = -\pi/5$. Parameters: $d = 1$, $g = 0.1J$, $|U| = 4J$, $2|\Delta_e| = 5.1J$.

2. Maybe I would omit the derivation of this dispersion relation as it does not compromise the readability of the paper, and there is already extensive literature showing how to derive those states e.g., J. Phys. B: At. Mol. Opt. Phys. 41 161002 (2008). Though, I leave this point with the authors' judgement.

Our reply: We thank the Reviewer for this valuable suggestion. The referenced work has now been cited in both the main text and the Supplementary Information. We put the detailed discussion of the repulsive case $U > 0$ in Supplementary Material Section I and II D (not shown in the main text).

Reviewer comments

3. I would ask the authors to simplify as much as possible the notation in this paper, as it really hinders the readability of the paper. For instance, I find the use of G^2 for the twophoton correlator a bit confusing since capital G is already used for the Green's function. Also, I *would suggest the authors checking whether there are symbols which are used in the main text yet not defined there. For example, after eq. 12 δ_k is not defined (and those equations lack the numbering) while being defined in the supplementary.*

Our reply:

We thank the Reviewer for the careful reading and the valuable feedback regarding notation clarity. We agree that consistent and clear notation is essential for readability, and we have taken the following steps to address the concerns raised:

1. **Simplification of redundant notation:**

   The quantities $f_K(n_1^\tau, n_2^\sigma)$ and $\vec{e}_{\tau\sigma}$ were previously defined separately but describe the same physical object. To avoid redundancy and improve clarity, we have removed the definition of $f_K(n_1^\tau, n_2^\sigma)$ entirely and now consistently use $\vec{e}_{\tau\sigma}$ throughout the main text and Supplement Information. On Page [3], the relevant section has been revised as follows:

   F_K is expressed as a sum over four decay channels:

   $$F_K = \sum_{\tau,\sigma} \vec{e}_{\tau\sigma}(K), \tag{R6}$$

   where each channel is represented as a complex vector to facilitate the interpretation of interference effects in subsequent sections. Each vector is defined as

   $$\vec{e}_{\tau\sigma}(K) = A_K\left(r_d^{\tau\sigma}\right) e^{i\phi_1^\tau} e^{i\phi_2^\sigma} e^{-iKx_c^{\tau\sigma}}, \tag{R7}$$

   with the amplitude

   $$A_K\left(r_d^{\tau\sigma}\right) = \sum_k \cos[(k - K/2) r_d^{\tau\sigma}] L_{k,K},$$
   $$L_{k,K} = \frac{2\sqrt{2}J}{N(\omega_k - \Delta_e)} \sum_m e^{-i(k-K/2)m} u_K(m),$$

   where $x_c^{\tau\sigma} = (n_1^\tau + n_2^\sigma)/2$, $r_d^{\tau\sigma} = n_1^\tau - n_2^\sigma$, $\delta_k = \omega_k - \Delta_e$ and $\omega_k = -2J\cos(k)$ is the single-photon dispersion relation.

   Accordingly, the original definitions in Eqs. (14) and (15) have been removed, and the surrounding text has been streamlined to maintain a clear logical progression.

2. **Explicit definition of previously undefined symbols:**

   - δ_k in $L_{k,K}$ is now defined after used:
     $\delta_k = \omega_k - \Delta_e$ and $\omega_k = -2J\cos(k)$ is the single-photon dispersion relation.
   - Δ_K in Eq. (10) is now defined after used:
     $\Delta_K = E_K - 2\Delta_e$

3. **Revised notation for the two-photon correlation function:**

   To prevent any potential confusion with the Green's function G, the two-photon spatial correlation function previously denoted as $G^{(2)}$ has been renamed as $\mathcal{G}^{(2)}$ throughout the text.

All relevant equations have also been properly numbered, and we have thoroughly verified that every symbol used in the main text is either defined or referenced clearly.

Reviewer comments

4. Eq. 16 is not trivial at all so I would ask to provide justification on its derivation

Our reply: We thank the Reviewer for this insightful comment. In the revised manuscript, we have expanded the logical derivation to enhance clarity. The key revisions are summarized as follows:

- **Introduction of the effective Hamiltonian for a single GEP:**

  We first explicitly present the effective interaction Hamiltonian for a single GEP on Page [3], following Eqs. (9) and (10). This establishes a clear physical foundation for extending the formalism to multiple GEPs.

  After adiabatically eliminating the single-photon intermediate state, we obtain the reduced two-photon state

$$|\psi(t)\rangle = \left[c_e(t)\sigma_1^+\sigma_2^+ + \sum_K c_K(t)\mathcal{D}_K^\dagger\right]|g, g, \mathrm{vac}\rangle. \tag{R8}$$

  From Eqs. (9) and (10), the effective interaction Hamiltonian between GEP and the nonlinear waveguide, i.e., the state $|e, e, \mathrm{vac}\rangle$ and $|g, g, K\rangle$ can be further derived as

$$H_{\mathrm{int}} = \frac{g^2}{J}\sum_{\tau,\sigma}\sigma_1^-\sigma_2^-\mathcal{D}^\dagger_{n_1^\tau,n_2^\sigma} + \mathrm{H.c.}, \tag{R9}$$

$$\mathcal{D}^\dagger_{n_1^\tau,n_2^\sigma} = \frac{1}{\sqrt{N_c}}\sum_K e^{i\Delta_K t} f_K(n_1^\tau, n_2^\sigma)\mathcal{D}_K^\dagger. \tag{R10}$$

  Note that, the operator $\mathcal{D}^\dagger_{n_1^\tau,n_2^\sigma}$ is defined in the interaction picture, which contains a time-depended phase factor.

- **Clarification of assumptions for the two-GEP network:**

  We then explicitly state the key assumptions for the two-GEP network: specifically, the separation condition $D_q \gg L_u(K)$, which suppresses supercorrelated radiation between emitters in different GEPs. Additionally, for the chosen initial state with only one GEP excited, we introduce the corresponding reduced two-photon state on Page [5].

We assume that the two GEPs have the same geometric layout but are separated by a distance D_q, with D_q sufficiently larger than $L_u(K_r)$. This ensures that supercorrelated emission between emitters in different pairs, i.e., the process $\langle \mathrm{vac}|\mathcal{D}_K^\dagger \sigma_{\mathrm{A},1/2}^- \sigma_{\mathrm{B},1/2}^- |\mathrm{vac}\rangle$, are suppressed. The operator $\sigma_{\alpha,i}^-$ denotes the lowering operator of emitter α_i. Under this condition, we consider the initial state:

$$|\psi(t=0)\rangle = \sigma_{\mathrm{A},1}^+ \sigma_{\mathrm{A},2}^+ |g, g, \mathrm{vac}\rangle,$$

which only GEP A is excited, and states $\sigma_{\mathrm{A},1/2}^- \sigma_{\mathrm{B},1/2}^- |g, g, \mathrm{vac}\rangle$ can be neglected. Accordingly, the reduced system state analogous to Eq. (13) becomes:

$$|\psi(t)\rangle = \left[\sum_\alpha c_e^\alpha(t) \sigma_{\alpha,1}^+ \sigma_{\alpha,2}^+ + \sum_K c_K(t) \mathcal{D}_K^\dagger \right] |g, g, \mathrm{vac}\rangle. \tag{R11}$$

Here, $\alpha =$ A, B denotes that supercorrelated radiation is confined within individual GEPs.

- **Generalization to the two-GEP interaction Hamiltonian:**

  Building on the single-GEP result, we generalize the interaction Hamiltonian for the two-GEP network on Page [5]:

  Analogous to Eq. (14), the interaction Hamiltonian can be expanded in the basis of Eq. (17) as

  $$H_{\mathrm{int}} = \frac{g^2}{J} \sum_\alpha \sum_{\tau,\sigma} \sigma_{\alpha,1}^- \sigma_{\alpha,2}^- \mathcal{D}_{n_{\alpha,1}^\tau, n_{\alpha,2}^\sigma}^\dagger + \mathrm{H.c.} \tag{R12}$$

  In contrast to Eq. (14), the labels now include an additional index $\alpha =$ A, B, where (α, i, τ) denotes the i-th emitter in pair α coupled to the waveguide at position $n_{\alpha,i}^\tau$

Reviewer comments

5. In eq. 17 the authors introduce a doublon state creation operator, which in the end is a time-dependent combination of what in the initial section were already called "doublons". I would ask the authors to clarify this point (also this dependency).

Our reply: We thank the Reviewer for careful reading and for identifying the imprecise description of the operator $\mathcal{D}_{n_1^\tau, n_2^\sigma}^\dagger$.

The operator $\mathcal{D}_{n_1^\tau, n_2^\sigma}^\dagger$ is not a doublon state creation operator. Instead, it is defined in the interaction picture and contains an explicit time-dependent phase factor $\exp i\Delta_K t$, where $\Delta_K = 2\Delta_e - E_K$ represents the frequency detuning. Consequently, referring to it as a "**doublon creation operator**" was inaccurate and potentially misleading.

To address this, we have made the following revisions to the manuscript:

1. We have removed the term "doublon creation operator" in reference to $\mathcal{D}_{n_1^\tau, n_2^\sigma}^\dagger$ and now refer to it simply as an operator.

2. We now introduce this operator earlier in the text, on Page [3] alongside Eqs. (9) and (10), as part of the derivation of the effective Hamiltonian for a single GEP, which clarifies its physical origin and mathematical form.

The revised description now reads:

Note that, the operator $\mathcal{D}^{\dagger}_{n_1^{\tau},n_2^{\varsigma}}$ is defined in the interaction picture, which contains a time-depended phase factor.

We hope this clarification eliminate the ambiguity.

Reviewer comments

6. Given the analogy with the results of Ref. S5 (in Supp. Mat.), I would ask the authors to briefly comment on analogies and differences between their proposal and the standard system in which, through proper time-dependent couplings, a single excitation can be deterministically transferred between different atoms. What could be an advantage of using the proposed setup (if there is any)?

Our reply:

We sincerely thank the Reviewer for raising this insightful question.

While both our protocol and the scheme in Ref. S5 [PRA 84, 042341 (2011)] utilize properly engineered time-dependent couplings to mediate excitation transfer, they are distinct in physical mechanism: conventional protocols employ single photons as information carriers, whereas our approach exploits doublons (two-photon bound states) to enable **joint two-excitation transfer**. This key difference allows our setup to transfer two-photon (two-qubit) quantum states between remote network nodes in **a single-step operation**, in contrast to standard methods, which are limited to transferring one excitation (one qubit) at a time.

This capability is particularly advantageous for distributing multi-emitter entangled states. For example, in existing protocols, such as *Deterministic multi-qubit entanglement in a quantum network* [Fig. 3, adopted from Nature 590, 571 (2021)] **transferring a 3-qubit GHZ state requires three sequential single-qubit transfer operations, together with plenty of local gate operations.** By contrast, our architecture, where two emitters per node collectively couples to a nonlinear waveguide, enables **entanglement state transfer in a single-step operation**. Thus, a two-qubit entangled state prepared at node A, such as

$$|\Psi_{\mathrm{A}}(t_0)\rangle = c_e^{\mathrm{A}}|e,e\rangle + c_g^{\mathrm{A}}|g,g\rangle,$$

can be mapped onto node B in a single step, preserving entanglement without intermediate operations.

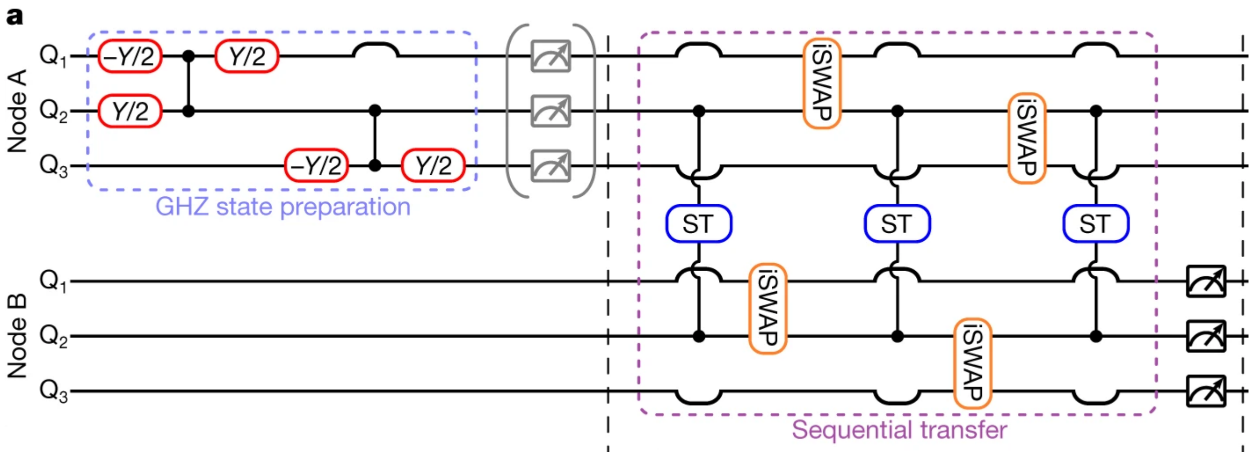

Figure R3. Schematic of the GHZ state preparation and the sequential state-transfer (ST) protocol in *Deterministic multi-qubit entanglement in a quantum network*. The figure is taken from *Nature 590, 571 (2021)*.

We have clarified this distinction on Page [6] of the revised manuscript by adding *Nature 590, 571 (2021)* as Ref [71]:

Unlike conventional multipartite entanglement transfer with single flying qubits [71], this nonlinear interface enables entanglement state transfer in a single-step operation. For example, an initial entangled state of GEP A, $|\Psi_{\rm A}(t_0)\rangle = c_e^{\rm A}|e,e\rangle + c_g^{\rm A}|g,g\rangle$, can be directly mapped onto GEP B as $|\Psi_{\rm B}(t_0)\rangle = c_e^{\rm B}|e,e\rangle + c_g^{\rm B}|g,g\rangle$ without sequential operations.

Reviewer comments

Minor comments 7. There are some typos: "direcional" on page 3, G^2 on Fig 4 caption etc

Our reply:

Thank the Reviewer for careful reading and for pointing out these typos. We have revised all of them.

Reviewer #2

Reviewer comments

This paper presents a scheme of directional generation of multiple-photon bound states using nonlinear waveguides of photons and giant emitters (GEs) that couple to different sites of the waveguide with different phases. The key ideas are: (1) bound states of multiple photons (in particular, dublons for two photons) are formed with center-of-mass momentum K; (2) Lower-photon emissions (such as single-photon emission) are virtual and can be adiabatically eliminated by setting the parameters such that the bound states of interest are within the gaps between the energy bands for the scattering states of different numbers of photons; (3) GEs have different pathways to generate the multi-photon bound states with c.o.m momentum K or -K (by energy conservation under the Markovian approximation for the dublon emission) and the interferenece between such pathways of emission, whose phases depend on c.o.m. momentum and the sites where the photon emission occurs, leads to the direction selection (K versus -K), defined as chirality C. A toy model consisting of a tight-binding 1D chain of cavities with on-site interaction (Hubbard type U) and two-level GEs each coupled to two cavities separated by distance d (=0, 1, etc). It is understandable such a simple model is empployed for a proof-of-the-principle study. The calculation shows that the chirality C in a quite large range of parameters is close to the perfect values +/- 1. The physics behind the calculation is well understood. The authors present a scheme of cascade quantum networks based on the directional generation of photon doublons. The scheme can be generalized to more-photon bound state. A scheme of generating multi-atom NOON state is also presented. Using realistic parameters of suoerconducting resonator systems that are currently available in laborratories, the authors demonstrate the feasibility of the schemes.

Our reply: We thank the Reviewer for giving a comprehensive summary of our work

Reviewer comments

The paper in general is clearly written. I recommend the acceptance of the paper after addressing the following points (some are quite minor):

Our reply: We sincerely thank the Reviewer for the positive assessment and for noting that the manuscript is clearly written. Below, we provide a point-by-point response to the Reviewer's comments and have revised the manuscript accordingly.

Reviewer comments

1. There are existing schemes of generating directional single photons or photons in coherent states using superradiance of atom ensembles (time-Dicked states), which can be understood as one-photon generating GE in some sense [see, e.g., PRA 91, 011801(R) (2015)]. For single photon states, of course, the nonlinear interaction between photons is not needed.

Such literature should be introduced.

Our reply:

We thank the Reviewer for pointing us to the relevant literature on directional single-photon generation via superradiance in atomic ensembles.

In response, we have added an introduction of generating directional single-photon research in the revised manuscript on Page [5].

Contrasting linear setups, such as interacting emitter pairs [6,7], multiple-level atoms [69], and superradiance of atom ensembles (time-Dicke states) [70], our proposal utilizes super-correlated photons as “flying qubits", enhancing numerous many-body applications.

Reviewer comments

2. In Eq. (2) and some other places, r (deinfed as $m-n$) is used to refer to the relative distance between two photons. But in most places of the paper, r_d is used (even including in Eq. (2)). The symbol should be unified.

Our reply:

We thank the Reviewer for careful reading and highlighting the inconsistency in notation. We have thoroughly revised the manuscript to ensure a unified notation throughout.

Specifically, we now consistently use $r_d = n_1 - n_2$ to denote the relative distance between two photons, while r is reserved for denoting the right coupling leg of giant emitters.

All relevant instances in the main text and Supplementary Material, including Eq. (2) and surrounding discussions, have been updated accordingly to ensure notational consistency and clarity.

Reviewer comments

3. Persentation of Fig. 2 is not clear enough. Fig. 2a needs more explaining - what are bars? What are the shadowed curves? Are are (1) and (2) and the arrows? In Fig. 2b, what is $c_{x_c,r_d}(t)$ (not defined)? What is the value of time t in the plot (since in the figure c is plot as a function of x_c and r_d, not t)? In Fig. 2d, what is the value of Δ_e (there are two in Fig. 2b & 2c)?

Our reply:

We thank the Reviewer for pointing out the ambiguities in the presentation of Fig. 2. We have thoroughly revised both the figure and its caption to improve clarity and address all the raised points. The specific revisions are as follows:

- **Fig. 2a**: The vertical bars represent a single photon emitted by one giant emitter at position n_1^l (n_2^r). The shaded curves depict the spatial profile of the intermediate single-photon state generated by the other emitter during the two-photon emission process. The symbols ① and ② denote the two giant emitters, which are coupled to the waveguide, as indicated by the black and red dashed arrows, respectively.

- **Fig. 2b**: The quantity $|c_{x_c,r_d}(t)|^2$ denotes the joint probability distribution of two photons with center-of-mass coordinate $x_c = (n_1 + n_2)/2$ and relative coordinate $r_d = n_1 - n_2$, where n_1 and n_2 are the lattice positions of two photons. The distribution is plotted at time $Jt = 600$, corresponding to the dashed vertical line in Fig. 2c, when the emitter population has largely decayed.
- **Fig. 2b**: The emitter detuning is set to $2\Delta_e = -5.1J$ (i.e., $\Delta_e = -2.55J$), which corresponds to the optimal condition for directional doublon emission, consistent with the parameters used in Fig. 2b.

All these clarifications have been incorporated into the revised caption of Fig. 2 on Page [4]

Directional emission of doublons. (a) Sketches of the dual transition processes described by $\vec{e}_{lr}$. Vertical bars indicate a single photon localized at n_1^l (n_2^r), while the shaded curves represent the spatial envelope of the intermediate single-photon state. Two giant emitters {①, ②} are coupled to the waveguide at positions marked by the black and red dashed arrows, respectively. (b) Two-photon joint probability distribution $|c_{x_c,r_d}(t)|^2$ at time $Jt = 600$ (dashed line in c) with $2\Delta_e = -5.1J$ (optimal emission point). $x_c = (n_1 + n_2)/2$ and $r_d = n_1 - n_2$ denote the center-of-mass and relative coordinates of two photons at sites n_1 and n_2. The two-point correlation function $\mathcal{G}^{(2)}(r_d)$ is also shown. (c) Time evolution of $|c_e(t)|^2$ for $2\Delta_e = -4.6J$ and $-5.1J$. (d) Chiral factor as a function of $\Phi_{1,2}^e = \phi_{1,2}^r - \phi_{1,2}^l$, with $2\Delta_K = -5.1J$. The coupling strength is set to $g = 0.1J$; other parameters are the same as in Fig. 1d.

Reviewer comments

4. C should be a predic function of Φ_1^e and Φ_2^e. Why does C change its sign when $\Phi_{1/2}^e$ change from $-pi$ to $+pi$ (increased by 2π) as shown in the diagonal regions in Fig. 2d?

Our reply:

We thank the Reviewer for this insightful question. The chiral factor C is indeed a periodic function of Φ_1^e and Φ_2^e, with a period of 2π. To better illustrate this periodicity across multiple Brillouin zones, in Fig. R4, we plot C over an extended phase range $[-2\pi, 2\pi]$.

The sign reversal of C along the diagonal regions of Fig. 2d results from quantum interference among the four decay channels mediated by the GEP. To clarify this behavior and explicitly identify the parameter regions where $C = 0$, we have expanded Sec. S II C in Supplementary Material and added two new subsections (Sec. II C 2 and II C 3). These additions provide a

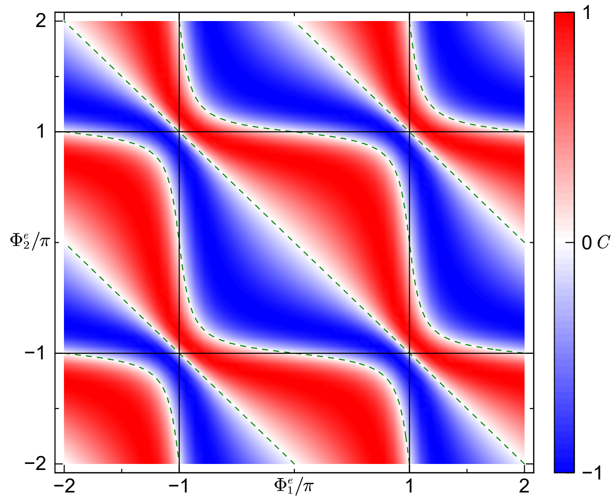

Figure R4. Chiral factor as a function of Φ_1^e and Φ_2^e, with $2\Delta_K = -5.1J$. The green dashed curves are given by (R22b) and (R22c). The coupling strength is set to $g = 0.1J$; other parameters are the same as in Fig. 2d.

detailed analytical treatment of how the sign of C is governed by Φ_1^e and Φ_2^e, and explicitly derive the nodal lines where the chiral factor vanishes.

C. Effects of the parameters of the GEP on decay and chiral

Equations (S45) and (S46) gives the analytical expressions of the decay rate and chiral factor, respectively. Leveraging these expressions, we now analyze how the geometric and coupling parameters of the GEP shape its dynamics.

2. Effects of the coupling phases and resonance frequency

We now focus on the case $D = 0$, and discuss how the coupling phases $\Phi_{1,2}^e$ and the resonance mode K_r (linked to the emitter frequency via $2\Delta_e = E_K$) shape GEP dynamics. In the main text, F_K is written as the sum of four vectors

$$F_K = \sum_{\tau,\sigma} \vec{e}_{\tau\sigma}(K), \tag{R13}$$

corresponding to the four decay channels in Fig. 3. Up to a global phase Φ_0, these vectors are:

$$\begin{aligned}
\vec{e}_{ll} &: A_{ll}, \\
\vec{e}_{lr} &: A_{lr}\, e^{i\Phi_2^e} e^{-iKd/2}, \\
\vec{e}_{rl} &: A_{rl}\, e^{i\Phi_1^e} e^{-iKd/2}, \\
\vec{e}_{rr} &: A_{rr}\, e^{i\Phi_1^e} e^{i\Phi_2^e} e^{-iKd},
\end{aligned}$$

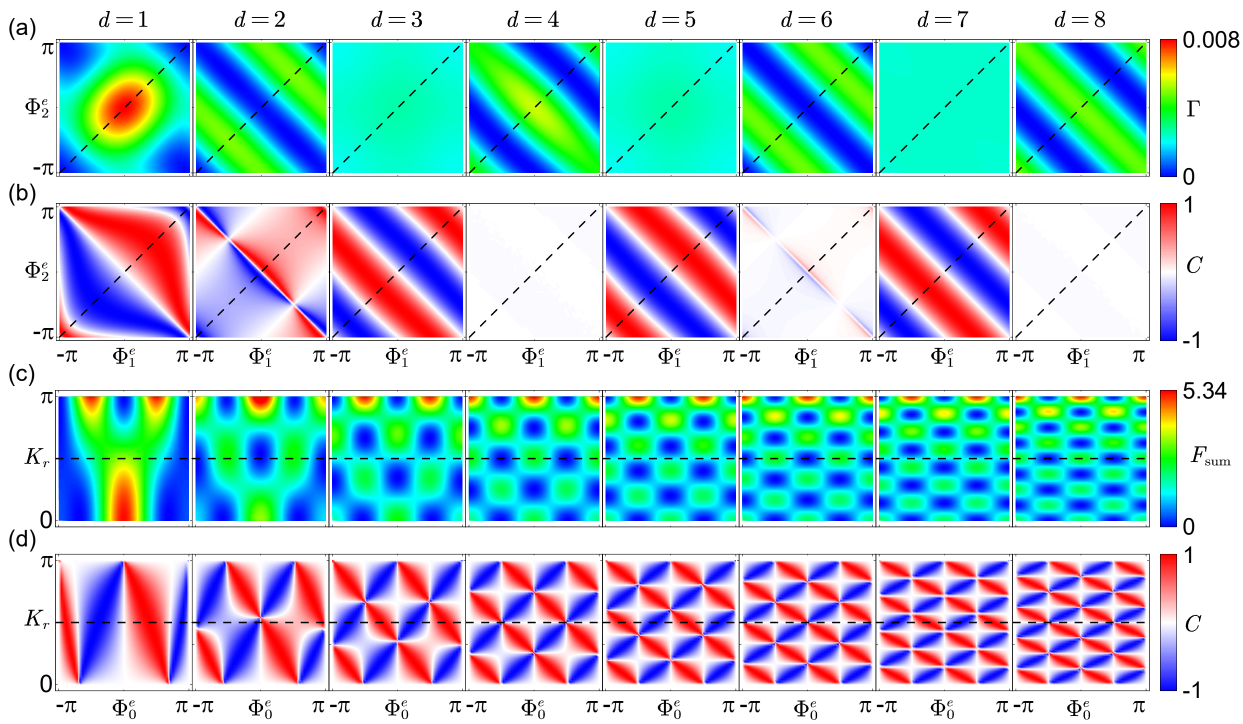

Figure R5. (a) Decay rate and (b) chiral factor, as functions of Φ_1^e and Φ_2^e for different giant-emitter sizes d, with $K_r = \pi/2$ ($\Delta_e = -2.61J$) indicated by the black dashed line in (c, d). (c) $F_{\text{sum}} = F(+K_r) + F(-K_r)$ and (d) chiral factor, as functions of K_r and $\Phi_0^e = \Phi_1^e = \Phi_2^e$ [anti-diagonal black dashed line in (a, b)]. The other parameters are the same as in Fig. 2 of the main text.

Owing to symmetry and $D = 0$, the amplitudes satisfy $A_{ll} = A_{rr} = A(0)$ and $A_{lr} = A_{rl} = A(d)$. Equation (S52) then simplified to

$$F(K) = A(0)\left[1 + e^{i\Phi_1^e} e^{i\Phi_2^e} e^{-iKd}\right] + A(d)\left[e^{i\Phi_2^e} + e^{i\Phi_1^e}\right] e^{-iK\frac{d}{2}}. \tag{R14}$$

From this expression, we derive

$$\begin{aligned}
&|F(+K)|^2 + |F(-K)|^2 = \\
&4A(0)^2\left[1 + \cos\left(\Phi_1^e + \Phi_2^e\right)\cos(2\theta)\right] + 8A(0)A(d)\cos(\theta)\left[\cos\left(\Phi_1^e\right) + \cos\left(\Phi_2^e\right)\right] \\
&+ 4A(d)^2[1 + \cos\left(\Phi_1^e - \Phi_2^e\right)],
\end{aligned} \tag{R15}$$

$$\begin{aligned}
&|F(+K)|^2 - |F(-K)|^2 = \\
&8A(0)\sin(\theta)\left\{A(0)\sin(\Phi_1^e + \Phi_2^e)\cos(\theta) + A(d)\left[\sin(\Phi_1^e) + \sin(\Phi_2^e)\right]\right\},
\end{aligned} \tag{R16}$$

where $\theta = Kd/2$.

In Fig. S5(a, b), we plot the decay rate Γ and chiral factor C as functions of Φ_1^e and Φ_2^e for different d, with $K = K_r = \pi/2$ [indicated by black dashed lines in Fig. S5(c, d)]. To isolate interference effects from dispersion-induced group velocity v_g [the denominator of the decay rate in Eq. (S45)], we analyze the sum amplitude $F_{\rm sum} = |F(+K)|^2 + |F(-K)|^2$ and C in the (K, Φ_0^e) plane, setting $\Phi_0^e = \Phi_1^e = \Phi_2^e$ [anti-diagonal in Fig. S5(a, b)]. Via the dispersion relation $2\Delta_e = E_K = -\sqrt{U^2 + 16J^2\cos^2(K/2)}$, the wavevector K directly maps to the emitter frequency.

We identify two distinct regimes:

1. Short separation ($d = 1$). All four channels contribute significantly. Both Γ and C reflect the interference among the four vectors.

2. Long separation [$d > L_u(K_r)$], where $A(d) \simeq 0$. The expressions Eqs. (S54) and (S55) reduce to

$$|F(+K)|^2 + |F(-K)|^2 \approx 4A^2(0)[1 + \cos(\Phi_+^e)\cos(Kd)], \tag{R17}$$
$$|F(+K)|^2 - |F(-K)|^2 \approx 4A^2(0)\sin(\Phi_+^e)\sin(Kd), \tag{R18}$$

   with the symmetric phase $\Phi_+^e = \Phi_1^e + \Phi_2^e$.

   In Fig. S5(a, b) ($K = \pi/2$), Γ and C exhibit pronounced interference patterns:

   - For Γ (panel a): When $\cos(Kd) = 0$ ($d = 3, 5, 7$), Γ becomes uniform. At $d = 4,\ 8$ [$\cos(Kd) = 1$], diagonal striped pattern appear, with alternating bright (green) and dark (blue) bands modulated by $\cos(\Phi_+^e)$; while the pattern inverts for $d = 6$ [$\cos(Kd) = -1$].
   - For C (panel b): When $\sin(Kd) = 0$ ($d = 4,\ 6,\ 8$), C vanishes. At $d = 3,\ 7$ [$\sin(Kd) = -1$], a similar striped pattern appears, with red (positive) and blue (negative) bands separated by nodal lines at $\sin(\Phi_+^e) = 0$ ($\Phi_+^e = 0, \pm\pi$); the contrast flips for $d = 5$ [$\sin(Kd) = 1$].

   In Fig. S5(c, d), the full (K, Φ_0^e) dependence is shown:

   - $F_{\rm sum}$ (panel c) displays a checkerboard-like pattern. Horizontal variations (in Φ_0^e) follow a cosine envelope, while vertical oscillations (in K) become denser with increasing d. The overall intensity grows with K due to the K-dependence of $A(0)$.
   - C (panel d) forms a diamond lattice of alternating red/blue domains, reflecting sine dependence on Φ_0^e and Kd. Similarly, as d increases, vertical oscillation (in K) become denser. Nodal lines (white) are given by $\sin(Kd) = 0$ or $\sin(\Phi_0^e) = 0$.

Moreover, the red (blue) regions in Fig. S5(b, d), corresponding to $C = +1$ ($C = -1$), identify optimal parameters for unidirectional emission: the optimal mode K (i.e., emitter frequency Δ_e) together with coupling phases Φ_1^e and Φ_2^e.

These complex interference results demonstrate that both the super-correlated decay rate Γ and chirality C can be engineered via the geometric parameters d and D, as well as the encoded phases $\Phi_{1,2}^e$, and resonance frequency $2\Delta_e$.

3. Nodal Conditions for the Chiral Factor

The chiral factor C vanishes when the right and left emission intensities balance, i.e., $|F(+K)|^2 - |F(-K)|^2 = 0$. In that scenario, the GEP dynamics recover the small atom behaviour, with non-directional emission [S2]. From Eq. (S55), this occurs when

$$\sin(\theta)\sin\left(\frac{\Phi_1^e + \Phi_2^e}{2}\right)\left[A(0)\cos\theta\cdot\cos\left(\frac{\Phi_1^e + \Phi_2^e}{2}\right) + A(d)\cos\left(\frac{\Phi_1^e - \Phi_2^e}{2}\right)\right] = 0. \tag{R19}$$

This condition is satisfied in three distinct scenarios:

$$\theta = \frac{Kd}{2} = m\pi, \quad m \in \mathbb{Z}, \tag{R20a}$$

$$\Phi_1^e + \Phi_2^e = 2m\pi, \quad m \in \mathbb{Z}, \tag{R20b}$$

$$A(0)\cos\theta\cdot\cos\left(\frac{\Phi_1^e + \Phi_2^e}{2}\right) + A(d)\cos\left(\frac{\Phi_1^e - \Phi_2^e}{2}\right) = 0. \tag{R20c}$$

- Equation (S59a), implies that for suitable separations and resonance modes $Kd = 2m\pi$, the system cannot support directional emission regardless of coupling phases, as shown in Fig. S5(b) for $d = 4,\ 6,\ 8$ and the horizontal white bands in Fig. S5(d).

- Equation (S59b), defines a diagonal line in the phase plane, independent of K or d, visible as a white diagonal in Fig. S5(b) and vertical white zones at $2\Phi_0^e = \Phi_1^e + \Phi_2^e = 0, 2\pi$ in Fig. S5(d).

- Equation (S59c), yields curved nodal lines depending on both K, d (via θ) and $A(d)$, accounting for the remaining white features in Fig. S5(b, d).

We hope this explanation, together with the supplementary analysis, resolves the Reviewer's concern.

Reviewer comments

5. Does the optimal Δ_e depend on d (the size of a GE)? If yeas, what is the value of Δ_e in Fig. s4 (which shows the dependence of chirality C on d)? Is it the same for all d's or optimized for each d?

Our reply:

We thank the Reviewer for this insightful question. Indeed, the optimal emitter frequency Δ_e depend on the size d of the GEP.

The optimal condition for chiral emission, corresponding to $|C| \to 1$, is achieved when either $F_{+K_r} = 0$ or $F_{-K_r} = 0$. Through the dispersion relation $2\Delta_e = E_{K_r}$, Δ_e maps directly to the resonant mode K_r. Furthermore, the amplitude F_{K_r} contains an accumulated propagation phase factor $e^{-iK_r x_c^{\tau\sigma}}$ that depends explicitly on both K_r and the spatial separation d between coupling points. Therefore, the interference condition that maximizes chirality and hence the optimal value of Δ_e varies with d.

In the original Fig. S4, we fixed $\Delta_e = -2.61J$ ($K_r = \pi/2$) for all d to illustrate how the decay rate and chirality evolve with increasing emitter size. To fully address the Reviewer's question, we have now added new panels [Fig. S4 (c, d)] in the Supplementary Material, which display C as a function of both the wavevector K (equivalently, Δ_e) and the coupling phase Φ_0^e. These plots explicitly show how the optimal Δ_e shifts with d. A corresponding paragraph has been added on Page [11] to discuss this dependence in detail.

Moreover, the red (blue) regions in Fig. S3(b, d), corresponding to $C = +1$ ($C = -1$), identify optimal parameters for unidirectional emission: the optimal mode K (i.e., emitter frequency Δ_e) together with coupling phases Φ_1^e and Φ_2^e.

For further context regarding Fig. S4(c,d), we refer the Reviewer to our response to the previous comment. We hope this clarification resolves the raised concern.

Reviewer comments

6. In Eq. (19), the decay rates are temporally modulated to optimize state transfer between different sites. Ref. [8] is cited for this. There were earlier works proposing such ideas, see, e.g., PRL 78, 3221 (1997) and PRL 95, 030504 (2005), which may be appropriate references.

Our reply:

We thank the Reviewer for this valuable suggestion and for pointing us to these seminal earlier works. In the revised manuscript, we have added citations to both of these foundational papers alongside Ref. [8] on Page [6].

Reviewer #3

Reviewer comments

In "Nonlinear cascaded quantum network with giant emitters" Wang et al. propose to combine giant emitters with nonlinear waveguides as a way to obtain directional emission of mutiphoton bound states for quantum network applications. As possible applications, they propose the long-distance transfer of an entangled Bell state and or the dissipative generation of multipartite entanglement. They briefly discuss the feasability of an implementation in circuit QED.

Our reply: We thank the Reviewer for giving a comprehensive summary of our work.

Reviewer comments

In my view, the present work builds upon the photon bound-state emission analysis presented in Ref. [49], employing the same approximations and arriving at an almost identical mathematical description of the emission process. The key difference is that, in the current case, the emission can be directional. This arises from the use of giant atoms, which couple to neighboring nodes with different phases—an effect that has been extensively studied in the literature on linear waveguides. The combination of this directionality (introduced by giant atoms) and the same approximations used in the master-equation derivation of Ref. [49] leads to a cascaded master equation involving multiple emitters. The authors identify this equation as equivalent to those previously shown to support remarkable applications in cascaded networks within linear waveguides, such as state transfer and entanglement distribution.

Our reply: We sincerely thank the Reviewer for the thoughtful assessment, which clearly articulates how our work builds upon Ref. [49] by incorporating giant atoms to achieve directional emission, leading to a cascaded master equation and enabling applications such as state transfer and entanglement distribution.

Reviewer comments

Clarity: The combination of these two setups—nonlinear waveguides and giant atoms—requires the reader to grasp two conceptually nontrivial ideas. However, the manuscript devotes only a very limited amount of space to explaining them. As a result, the paper could be made significantly clearer and easier to follow if the authors expanded these sections and provided a more detailed discussion of the underlying concepts.

Our reply: We thank the Reviewer for this valuable suggestion regarding the clarity of our manuscript.

We fully agree that combining nonlinear waveguide QED with the giant-atom configuration involves two conceptually rich frameworks, which may present challenges to readers unfamiliar with either topic. In response to this comment, we have significantly expanded the Introduction (Page [1]) to provide a more accessible overview.

Specifically, the added second paragraph provides a clearer explanation of nonlinear waveguides, emphasizing how on-site photon-photon interactions lead to correlated photon-pair emission. The third paragraph introduces the concept of giant atoms, highlighting how multiple coupling points lead to quantum interference and enable directional emission. These revisions are intended to provide readers with the essential physical intuition to better understand the main results presented in the paper.

Recent progress in engineered quantum platforms has opened promising pathways toward overcoming this challenge, such as superconducting circuit QED via the intrinsic anharmonicity [25-27] or Rydberg atom arrays via dipole blockade [28,29]. A notable example is provided by nonlinear waveguides, which are often modeled by Bose–Hubbard Hamiltonians with on-site photon-photon interactions [30-33]. In such systems, the interplay between nonlinearity and dispersion leads to strongly correlated multiphoton states, where photons can become bound together in real space [34-37]. These correlated states, in turn, can mediate supercorrelated radiation dynamics and enable the generation of correlated photon pairs [38-42].

In parallel, the emerging paradigm of giant atoms has attracted considerable attention [43-47]. A giant atom couples to a photonic or phononic bath at multiple discrete points, with an effective size comparable to the operating wavelength [48-54]. This multi-point coupling structure gives rise to multiple decay channels that interfere quantum mechanically. By engineering the geometry and phase of these coupling points, one can tailor the interference to facilitate novel phenomena such as decoherence-free dipole-dipole interactions [55-58], oscillating bound states [59-62], and chiral quantum effects [63-65].

We hope these enhancements make the manuscript clearer and easier to follow.

Reviewer comments

Novelty and relevance: I find the idea of combining giant atoms with nonlinear waveguides novel and potentially interesting. However, its relevance to the field of quantum networks is not at all clear. To the best of my knowledge, directional emission of correlated photons can already be achieved using linear waveguides. For example, this can be realized with two directly interacting emitters, or with a single emitter possessing multiple energy levels or enabling two-photon transitions. It would therefore be important for the authors to clarify what specific advantages from introducing nonlinear waveguides, as opposed to the well-studied linear systems that already support cascaded quantum networks.

Our reply: We sincerely thank the Reviewer for this insightful comment and for recognizing the novelty of combining giant atoms with nonlinear waveguides. We appreciate the opportunity to further clarify the specific advantages and relevance of our approach compared to well-studied linear-waveguide schemes.

We have extensively revised the manuscript to address this point. The key additions and adjustments are summarized as follows.

1. **Clarifying the limitations of linear cascaded networks and our advance.**

   As the Reviewer rightly notes, directional emission of single photons or correlated photons can indeed be achieved in linear systems. However, those in linear system and our proposal are distinct in physical mechanism: conventional protocols employ single photons as information carriers, whereas our approach exploits doublons (two-photon bound states) to enable **joint two-excitation transfer**. This key difference allows our setup to transfer two-photon (two-qubit) quantum states between remote network nodes in **a single-step operation**, in contrast to standard methods, which are limited to transferring one excitation (one qubit) at a time.

   This capability is particularly advantageous for distributing multi-emitter entangled states. For example, in existing protocols, such as *Deterministic multi-qubit entanglement in a quantum network* [Fig. 3, adopted from Nature 590, 571 (2021)] **transferring a 3-qubit GHZ state requires three sequential single-qubit transfer operations, together with plenty of local gate operations.** By contrast, our architecture, where

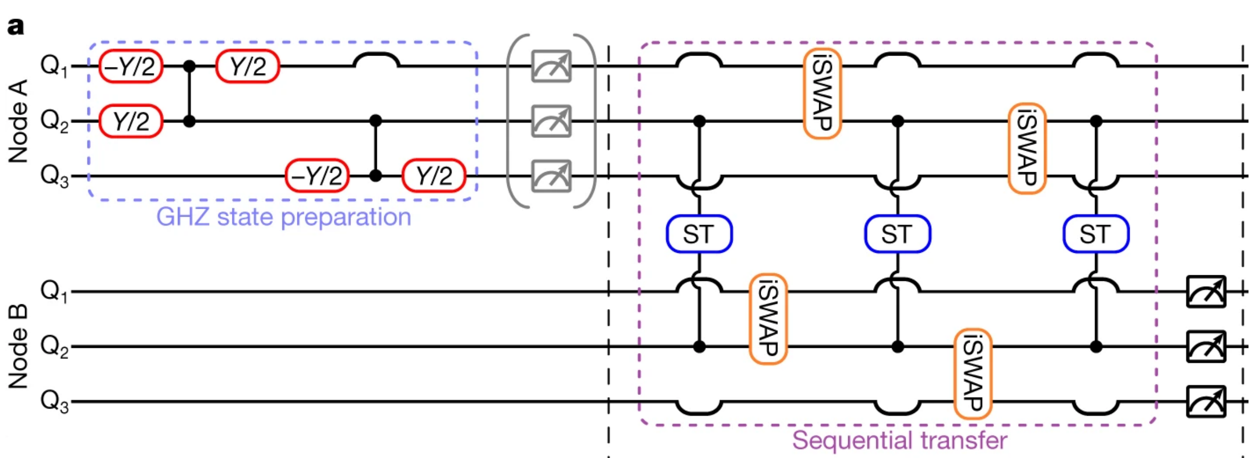

Figure R6. Schematic of the GHZ state preparation and the sequential state-transfer (ST) protocol in *Deterministic multi-qubit entanglement in a quantum network*. The figure is taken from *Nature 590, 571 (2021)*.

   two emitters per node collectively couples to a nonlinear waveguide, enables the **direct and simultaneous transfer of two correlated excitations**. Thus, a two-qubit entangled state prepared at node A, such as

$$|\Psi_{\rm A}(t_0)\rangle = c_e^{\rm A}|e,e\rangle + c_g^{\rm A}|g,g\rangle,$$

can be mapped onto node B in a single step, preserving entanglement without intermediate operations.

To clearly frame this distinction, we have first added an introduction of generating directional single-photon research in the revised manuscript on Page [5].

Contrasting linear setups, such as interacting emitter pairs [6,7], multiple-level atoms [69], and superradiance of atom ensembles (time-Dicke states) [70], our proposal utilizes supercorrelated photons as “flying qubits", enhancing numerous many-body applications.

We have also clarified this distinction on Page [6] of the revised manuscript by adding *Nature 590, 571 (2021)* as Ref [71]:

Unlike conventional multipartite entanglement transfer with single flying qubits [71], this nonlinear interface enables entanglement state transfer in a single-step operation. For example, an initial entangled state of GEP A, $|\Psi_{\mathrm{A}}(t_0)\rangle = c_e^{\mathrm{A}}|e,e\rangle + c_g^{\mathrm{A}}|g,g\rangle$, can be directly mapped onto GEP B as $|\Psi_{\mathrm{B}}(t_0)\rangle = c_e^{\mathrm{B}}|e,e\rangle + c_g^{\mathrm{B}}|g,g\rangle$ without sequential operations.

2. **Highlighting the broader implications for network architecture.**

   To better connect our work with quantum network, we have restructured the end of Section “Nonlinear Cascaded Quantum Network” to emphasize the nonlinear cascaded master equation. In particular, we have also added a concluding summary on Page [7]

   Following the methods in Fig. [4], our proposal enable single-step transfer of an arbitrary $\mathcal{N}$-qubit GHZ state, $|\psi_0\rangle = c_e|e\rangle^{\otimes\mathcal{N}} + c_g|g\rangle^{\otimes\mathcal{N}}$, between two $\mathcal{N}$-body nodes, without decomposing it into sequential single-excitation processes. In summary, our work demonstrates that nonlinear waveguides can be configured as multiphoton buses supporting advanced many-body quantum applications in future study.

Our work thus establishes nonlinear waveguides as a promising platform for quantum buses, unlocking potential applications inaccessible to linear waveguides. We hope the revised manuscript now more clearly highlights the distinctness of our proposed nonlinear cascaded quantum network. We thank the Reviewer again for prompting the comparison with prior literature in linear waveguide, which has also helped us better recognize and present the advantages of our approach.

Reviewer comments

Leaving aside this major point, I have a few additional comments and questions:

Our reply: We thank the Reviewer for these insightful comments. We have carefully considered each suggestion and have revised the manuscript accordingly. Our point-by-point responses are provided below.

Reviewer comments

-Can the choice of phases be adjusted to recover the non-directional emission discussed in Ref. [49]? Addressing this point (for example, in page 4 when directional emission is introduced) would help strengthen the conceptual link between the present results and those of Ref. [49].

Our reply:

We thank the Reviewer for this valuable suggestion, which helps to clarify the connection between our work and Ref. [49]. Indeed, in our proposal, when the chiral factor vanishes, i.e.,

$$|F(+K)|^2 - |F(-K)|^2 = 0,$$

the emission behavior of the CEP recovers that of a small atom, exhibiting the non-directional emission characteristic of Ref. [49].

To clearly identify the parameter regimes leading to this condition, we have added a new subsection (Section II.C.3 *"Nodal Conditions for the Chiral Factor"*) in the Supplementary Material on Page [11], which provides an analytical derivation of the requirement for $C = 0$

3. Nodal Conditions for the Chiral Factor

The chiral factor C vanishes when the right and left emission intensities balance, i.e., $|F(+K)|^2 - |F(-K)|^2 = 0$. In that scenario, the GEP dynamics recover the small atom behaviour, with non-directional emission [S2]. From Eq. (S55), this occurs when

$$\sin(\theta)\sin\left(\frac{\Phi_1^e+\Phi_2^e}{2}\right)\left[A(0)\cos\theta\cdot\cos\left(\frac{\Phi_1^e+\Phi_2^e}{2}\right)+A(d)\cos\left(\frac{\Phi_1^e-\Phi_2^e}{2}\right)\right]=0. \tag{R21}$$

This condition is satisfied in three distinct scenarios:

$$\theta = \frac{Kd}{2} = m\pi, \quad m \in \mathbb{Z}, \tag{R22a}$$

$$\Phi_1^e + \Phi_2^e = 2m\pi, \quad m \in \mathbb{Z}, \tag{R22b}$$

$$A(0)\cos\theta\cdot\cos\left(\frac{\Phi_1^e+\Phi_2^e}{2}\right)+A(d)\cos\left(\frac{\Phi_1^e-\Phi_2^e}{2}\right)=0. \tag{R22c}$$

- Equation (S59a), implies that for suitable separations and resonance modes $Kd = 2m\pi$, the system cannot support directional emission regardless of coupling phases, as shown in Fig. S5(b) for $d = 4,\ 6,\ 8$ and the horizontal white bands in Fig. S5(d).

- Equation (S59b), defines a diagonal line in the phase plane, independent of K or d, visible as a white diagonal in Fig. S5(b) and vertical white zones at $2\Phi_0^e = \Phi_1^e + \Phi_2^e = 0, 2\pi$ in Fig. S5(d).

- Equation (S59c), yields curved nodal lines depending on both $K,\ d$ (via θ) and $A(d)$, accounting for the remaining white features in Fig. S5(b, d).

Furthermore, in the main text on Page [5], we have incorporated a discussion following the introduction of directional emission, explicitly linking our results to the non-directional case discussed in Ref. [49].

In the white region where $C = 0$, the GEP dynamics recover the small-atom behaviour with non-directional emission [38]. The specific parameter regimes corresponding to $C = 0$ are discussed in Section II C of Supplementary Material.

We believe these additions effectively strengthen the conceptual connection between the two works and thank the Reviewer again for the valuable suggestion.

Reviewer comments

-What is the main source of imperfection that limits the reported fidelity to 98%, rather than 100%?

Our reply: We thank the Reviewer for this insightful question regarding the origin of the fidelity limitation in our state transfer protocol.

The achieved fidelity of approximately 98% (as opposed to 100%) is primarily limited by the following physical and practical factors:

- **Intermediate single-photon process:** Prior to supercorrelated radiation, the dynamics involve population of intermediate single-photon states, as shown by the shadowed curves in Fig. 2(a). The non-ideal spontaneous emission characteristics during this intermediate stage slightly perturb the ideal evolution required for perfect state transfer.

- **Finite time window:** Theoretically, perfect state transfer requires modulation pulses extending from $t \to -\infty$ to $t \to +\infty$. In our numerical simulation, however, we necessarily employ a finite time window, which introduces minor deviations from the perfect fidelity.

To address this point, we have added the following clarification in the revised manuscript on Page [6]:

At the final time t_f, one finds that $\{|c_e^{\mathrm{A}}(t_f)|^2, \sum_K |c_K(t_f)|^2\} \simeq 0$, and the absorption efficiency is $|c_e^{\mathrm{B}}(t_f)|^2 \simeq 98\,\%$. This value is primarily limited by the finite simulation time window and the non-ideal spontaneous emission dynamics during the single-photon intermediate process.

We hope this explanation addresses the Reviewer's question.

Reviewer comments

-The use of the term "intriguing" in this context does not seem appropriate for a scientific manuscript, in my opinion. A more precise and descriptive characterization of the result would be preferible.

Our reply: We thank the Reviewer for the valuable suggestion regarding the use of subjective language. In response, we have removed the term "intriguing" throughout the manuscript and replaced it with more precise and objective phrasing. The two specific instances have been revised as follows:

- We now demonstrate a high-fidelity process for entangled-state transfer...
- We further consider an application in which the three GEs in two remote nodes are pumped via three-photon parametric down-conversion processes...

Reviewer comments

-The paragraph on experimental feasibility appears to closely follow that of Ref. [49], suggesting that an independent evaluation may not have been performed. It would be useful if the authors could comment on the coupling strengths (g values) reported in the cited giant-atom experiments and discuss whether these are consistent with the parameters used in their simulations.

Our reply:

We thank the Reviewer for this important point regarding experimental feasibility and for prompting a more independent evaluation. In response, we have thoroughly revised the corresponding section on Page [7] to provide a dedicated evaluation of the experimental parameters relevant to giant atoms.

Our proposal is feasible in circuit-QED systems [27,75,76]. An array of coupled transmon qubits [25] can be configured as the nonlinear waveguide. The hopping rate and Kerr nonlinearity of such an array demonstrated in experiments [30,77-79] are on the order of $J/2\pi \sim 50\,\mathrm{MHz}$ and $U/2\pi \sim 200\,\mathrm{MHz}$, respectively.

The giant-atom configuration, with multiple discrete coupling points to a waveguide, has already been experimentally realized in Refs [52,56]. In our scheme, the relative coupling phases required for directional emission can be dynamically tuned via parametric modulation [65]. The transmon anharmonicity $U_{\mathrm{giant}}/2\pi \sim 300\,\mathrm{MHz}$ supports the two-level approximation for the emitters. Furthermore, time-dependent interactions between superconducting giant atoms and the nonlinear waveguide can be realized using methods from Ref. [65,80], achieving a coupling strength of $g/2\pi = 0.1J/2\pi \sim 5\,\mathrm{MHz}$.

Under these parameters, the supercorrelated emission rate is estimated as $\Gamma_{\pm}/2\pi \sim 1\,\mathrm{MHz}$ (see Supplementary Materials), which is much larger than the intrinsic decoherence rate of a circuit-QED platform [81,82]. Therefore, the phenomena predicted in this work are possible to observe in current circuit-QED setups.

CONCLUSION

In conclusion, we really thank the Reviewers for very useful comments and constructive criticism. Those comments help us improve the paper significantly. We have addressed all comments in the revised manuscript and highlighted the changes there. We hope the Reviewers now find our paper ready for publication in Communications Physics.

Yours sincerely,

the authors

RESPONSE LETTER TO REVIEWERS

Reviewer #1

Reviewer comments

- Entanglement transfer with linear waveguides -

To my comment on the novelty and relevance, the authors respond that "conventional methods are limited to transfer one excitation at a time". However, they also say "As the Reviewer rightly notes, directional emission of single photons or correlated (I assume multiphoton?) photons can indeed be achieved in linear systems". These two statements appear internally inconsistent and require clarification.

If the authors believe that nonlinear waveguides provide an "alternative" route for entanglement state transfer in a single-step operation, then they should explicitly acknowledge and cite existing approaches based on linear waveguides that achieve comparable functionality, and clearly position their method as an alternative within this broader landscape. Conversely, if the authors claim that nonlinear waveguides constitute the only known approach (to the best of current knowledge) enabling entanglement state transfer in a single-step operation, this claim should be stated explicitly.

At present, the manuscript remains too vague on this point. For instance, the authors write: "Unlike conventional multipartite entanglement transfer with single flying qubits, this nonlinear interface enables entanglement state transfer in a single-step operation"

-Do linear waveguides support emission of two-photon states? If yes, then it seems that entanglement-transfer is also possible using linear waveguides. For example Ref.[69] suggests that multi-photon emission is possible with linear waveguides.

Our reply: We thank the Reviewer for this insightful comment. In a quantum network, both the "flying qubits" and the structure of each quantum node determine the class of quantum information protocols that can be implemented.

We agree that linear waveguide QED setups, such as the multiphoton emission scheme in Ref. [69], can generate correlated photon pairs from a single multi-level emitter. However, in such approaches, the multi-level atom is effectively described as a single effective two-energy-level qubit via adiabatic elimination of the intermediate state. Consequently, the quantum node does not host genuine multipartite entanglement among multiple stationary qubits, and cannot support protocols requiring pre-engineered many-body states (e.g., GHZ states) to be transferred between remote nodes.

In contrast, our scheme operates in the multi-excitation manifold of multiple stationary qubits and enables the transfer of genuine GHZ-type entanglement, as detailed in the following response regarding the advantages over linear-waveguide approaches.

To clarify this point, we have added the following paragraph from Pages 6 to 7:

In linear waveguide QED setups, a single multi-level emitter can be adiabatically reduced to a single effective qubit for correlated-photon emission [69]. Since such a node lacks internal multipartite structure, it cannot support the **direct** transfer of many-body entangled states (e.g., GHZ states) between distant nodes.

Reviewer comments

-Also, it is not at all clear to me that single photons cannot be used for entanglement transfer. In quantum memories based on atomic ensembles, doesn't a single photon generate a multipartite entangled state in the atoms?

Our reply: We thank the Reviewer for this important point. It is true that a single photon can generate multipartite entanglement in atomic ensembles, for example, a **single-excitation W state** via collective absorption. However, such states belong to a different entanglement class than the **GHZ-type states** considered in our work. Crucially, W and GHZ states cannot be interconverted via local operations and classical communication (LOCC), and they exhibit fundamentally distinct properties (e.g., robustness to particle loss vs. maximal nonlocality). As the reply to the next comment, our scheme enables **deterministic transfer** of GHZ-type entanglement without any local operation.

Reviewer comments

Similarly, the statement "Contrasting linear setups,..., our proposal utilizes supercorrelated photons as "flying qubits", enhancing numerous many-body applications" is too vague. The manuscript should explicitly identify which many-body applications are enhanced and explain how the use of supercorrelated photons provides a concrete advantage over linear-waveguide-based approaches.

Our reply: As we wrote in previous reply, existing protocols, such as GHZ-state entanglement transfer in a linear quantum network [Fig. R1, adopted from Nature 590, 571 (2021)], requires sequential single-qubit transfer operations, together with plenty of local gate operations. To the best of our knowledge, our architecture is the first to enable **deterministic, single-step transfer of a pre-engineered GHZ state between multi-emitter nodes using correlated flying photonic states**.

Therefore, we thank the Reviewer for helping us find the suitable position of our research within the existing literature. Accordingly, we have revised the manuscript on Page 7 as

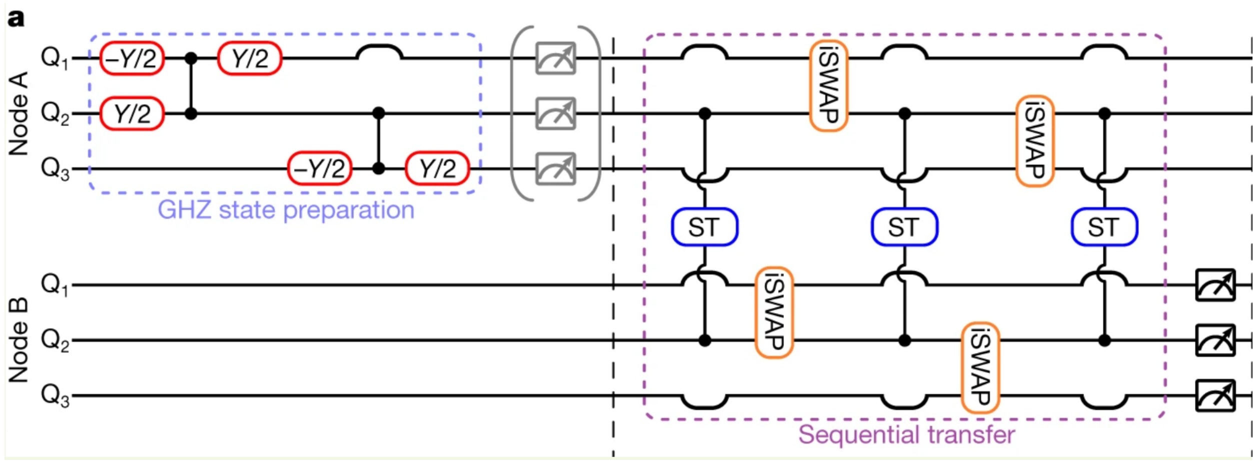

Figure R1. Schematic of the GHZ state preparation and sequential state-transfer (ST) protocol in deterministic multi-qubit entanglement distribution. The figure is reproduced from Nature **590**, 571 (2021) for peer-review purposes only.

follows:

Unlike conventional GHZ-state distribution in linear waveguides [71], which requires sequential single-photon transmissions and numerous local operations, our nonlinear cascaded interface accomplishes this many-body task without the need for sequential control or post-processing. For example, an initial entangled state of GEP A, $|\Psi_{\mathrm{A}}(t_0)\rangle = c_e^{\mathrm{A}}|e,e\rangle + c_g^{\mathrm{A}}|g,g\rangle$, can be directly mapped onto GEP B as $|\Psi_{\mathrm{B}}(t_0)\rangle = c_e^{\mathrm{B}}|e,e\rangle + c_g^{\mathrm{B}}|g,g\rangle$ in a single-step operation.

Reviewer comments

- 98% fidelity -

In response to my question regarding the dominant sources of imperfection, the authors state that the error arises from (1) finite transfer time and (2) intermediate single-photon processes.

The authors should quantify the relative contributions of these two mechanisms to the reported 2% infidelity. In my understanding, the error associated with (1) can reduced by increasing the transfer time. In contrast, the imperfection arising from (2) seems more fundamental, as it is intrinsic to the dynamics and may require modification of system parameters or operating regimes to mitigate.

The manuscript would benefit from a discussion addressing how each error contribution can be reduced. For example, are there parameter regimes in which these intermediate single-photon processes are further suppressed ? Clarifying whether this source of imperfection sets

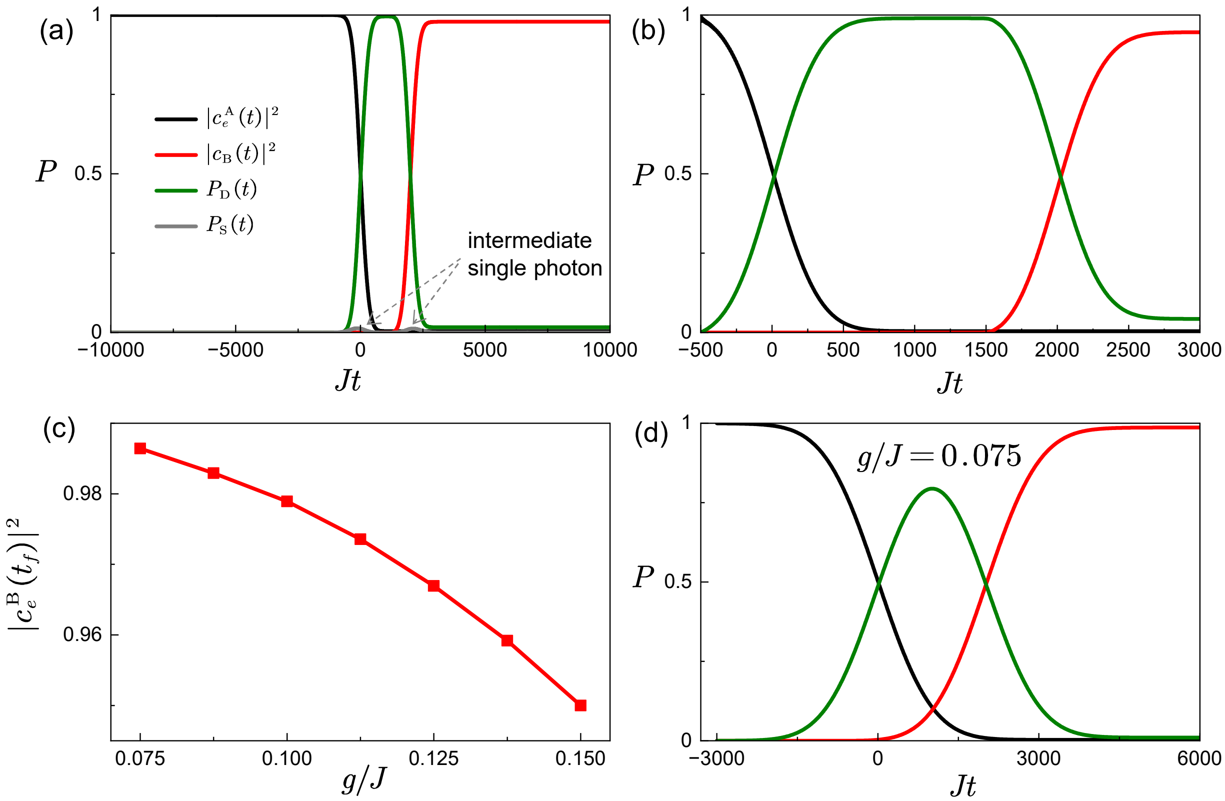

Figure R2. (a,b) State-transfer process under a longer ($t \in [-10000, 10000]$) and a shorter ($t \in [-500, 3000]$) time window compared to the main text ($t \in [-1500, 3000]$), with coupling $g/J = 0.1$. The gray curve indicates intermediate single-photon population $P_{\mathrm{S}}(t) = \sum_{m,k} |c_{mk}(t)|^2$. (c) Fidelity as a function of g/J. (d) State-transfer process for a weaker coupling $g/J = 0.075$. Other parameters are the same as in Fig. 4 of the main text.

a fundamental limit, or whether it can be engineered away, is essential for assessing the scalability and practical relevance of the proposal.

Our reply:

We thank the Reviewer for prompting us to clarify the sources of infidelity.

The error from source (1) can be suppressed by adopting a longer time-window. In Fig. R2(a), we take a sufficiently long time-window, $t \in [-10000, 10000]$, to suppress the infidelity from (1) as much as possible. The resulting fidelity of is only slightly higher ($\sim 0.1\%$) than the reported in the main text, confirming that the time window used ($t \in [-1500, 3000]$) is already long enough for the transfer process. Therefore, nearly all the 2% infidelity reported in the main text (Fig. 4) stems from the intermediate single-photon states. In contrast, for a shorter time window $t \in [-500, 3000]$ in Fig. R2(b), the fidelity decreases to 95%. Further discussion of this imperfection mechanism can be found in Phys. Rev. B **84**, 014510 (2011) and Phys. Rev. A **84**, 042341 (2011).

We now discuss source (2). In our analytical derivations, we assume that Δ_e is strongly detuned from the single-photon scattering states, which strongly suppresses the single-photon probability amplitudes. This enables us to adiabatically eliminate c_{mk} by assuming $\dot{c}_{mk}(t) = 0$, i.e.,

$$c_{mk}(t) \simeq -\left[\sum_{\tau=l,r} \frac{g}{\delta_k\sqrt{N}} e^{-ikn^{\tau}_{m'}} e^{i\phi^{\tau}_{m'}} c_e(t) + \sum_K \frac{g}{\delta_k} e^{-i\phi^{\tau}_m} M(k, n^{\tau}_m, K) c_K(t)\right]. \tag{R1}$$

In the ideal limit, $c_{mk}(t) = 0$. However, in practice [gray curves in Fig. R2(a)], $c_{mk}(t)$ is not identically zero. Such far-detuned emitter dynamics has been extensively studied, for example, in Phys. Rev. A 93, 033833 (2016), Phys. Rev. A 96, 043811 (2017) and related works. These intermediate single-photon states affect doublon emission and consequently the overall state-transfer fidelity.

From Eq. (R1), reducing the coupling strength g can suppress the intermediate single-photon states amplitudes and thus the error from (2). Fig. R2(c) shows that the fidelity increases as g decreases. However, the decay rate of the emitter [Eq. (16) in the main text] is given by

$$c_e(t) = \exp\left(-\frac{\Gamma_+ + \Gamma_-}{2} t\right), \quad \Gamma_\pm = \frac{g^4}{v_g J^2} \left|F_{\pm K_r}\right|^2, \tag{R2}$$

which scales as g^4. Therefore, reducing g significantly lengthens the required state-transfer time-window, as shown in Fig. R2(d) for $g/J = 0.075$, where $t \in [-3000, 6000]$ is twice as long as for $g/J = 0.1$. Thus, while intermediate single-photon contributions can be suppressed through parameter engineering, their complete elimination would require infinitely long transfer times—an unphysical condition in any real experiment.

In conclusion, suppressing both sources of infidelity, the intermediate single-photon states and the finite transfer time, requires increasing the transfer duration. However, a longer transfer time not only slows down the quantum information protocol but also allows other decoherence channels to become significant. Therefore, this trade-off leads to an optimal transfer time for realistic experimental implementations.

To clarify this point, we have revised the discussions on Page 6 as follows:

This value is primarily limited by the intermediate single-photon process and the finite transfer time [9]. Reducing the coupling strength during state transfer suppresses the intermediate single-photon amplitudes, thereby improving the corresponding fidelity. However, it also reduces the doublon emission rate, leading to a longer transfer time. This not only slows down the quantum information protocol but also enhances the impact of other decoherence channels. Consequently, in a realistic experimental implementation, an optimal coupling strength $g(t)$ might be chosen to balance transfer fidelity with operation speed.

We thank the Reviewer again for this helpful comment, which has allowed us to present the infidelity analysis more clearly.

Reviewer comments

Also, I do not understand the use of the term "simulation" in "finite simulation time window". I understand the authors refer an error due to finite transfer time. This will also appear in real setups and does not have to do with specifics of the numerical simulation.

Our reply:

We thank the Reviewer for this comment regarding the terminology. To accurately reflect the physical nature of this error source, we have revised the manuscript accordingly, replacing "finite simulation time window" with "finite operation time" or "finite transfer time" throughout the text.

Reviewer comments

— The dark state condition — "Because dark-state conditions always hold in this nonlinear cascaded system, the correlated-two-photon field is trapped between the two GEPs without leaking outside" In the context of quantum-state transfer, modulation of the light-matter coupling is needed in order to satisfy a "dark state condition" and thus achieve perfect transfer. To state that "dark-state conditions always hold in this nonlinear cascaded system" is confusing since it suggests modulation is not needed to achieve perfect transfer.

Our reply:

We thank the Reviewer for this clarification. We agree that the dark-state condition relies on the engineered time-dependent decay rates specified in Eq. (20). The original wording was misleading, and we have revised it accordingly. We revised the sentence on Page 6

Given that the decay rates are modulated according to Eq. (20), the dark-state conditions hold in this nonlinear cascaded system, and the correlated-two-photon field is trapped between the two GEPs without leaking outside.

CONCLUSION

We thank the Reviewer again for his/her careful reading of our manuscript, and for the useful comments and constructive criticism. We have addressed all the comments in the revised manuscript and highlighted the changes there. We hope the Reviewer now finds our paper ready for publication in Communications Physics.

Yours sincerely,

the authors

The work by Wang et al (number COMMSPHYS-25-1042-T) studies the problem of two-legged giant atoms weakly- coupled to a non-linear homogeneous coupled cavity array, in which a bound-photon minibands exist regardless of the sign of the interaction. For instance, in case of two giant atoms (so called "giant emitter pair" GEP), both resonant to the miniband, the authors discuss a mechanism for chiral emission of bound photon pairs, which is resilient to different geometric configurations of the giants, phase differences in the coupling etc. Building on that, together with technique of optimal control in time of the coupling strengths, the authors propose a so-called non-linear cascaded network, in which excitations can be deterministically transferred between different GEPs, or entanglement can be efficiently created between remote GEPs. In the end, the authors argue that this mechanism can be extended to configurations in which more than two photons are involved and discuss potential implementations within the paradigm of circuit-QED.

While the idea is potentially interesting, bridging non-linear systems with waveguide-QED, I cannot recommend it for publication before the authors have addressed the following points.

1. When introducing the model of a non-linear coupled cavity array, the authors discuss and derive the dispersion law of the miniband of bound photons, see Eq. 5. This result though only holds when U<0 (attractive interaction), as correctly stated in the supplementary material. In general, since the sign of the interaction seems not to be so important for the discussed phenomenology, I would amend this part by including both solutions (or else justify why they need U<0 for everything to work).
2. Maybe I would omit the derivation of this dispersion relation as it does not compromise the readability of the paper, and there is already extensive literature showing how to derive those states e.g., *J. Phys. B: At. Mol. Opt. Phys.* **41** 161002 (2008). Though, I leave this point with the authors' judgement.
3. I would ask the authors to simplify as much as possible the notation in this paper, as it really hinders the readability of the paper. For instance, I find the use of G^2 for the two-photon correlator a bit confusing since capital G is already used for the Green's function. Also, I would suggest the authors checking whether there are symbols which are used in the main text yet not defined there. For example, after eq. 12 δ_k is not defined (and those equations lack the numbering) while being defined in the supplementary.
4. Eq. 16 is not trivial at all so I would ask to provide justification on its derivation.
5. In eq. 17 the authors introduce a *doublon state creation* operator, which in the end is a time-dependent combination of what in the initial section were already called "doublons". I would ask the authors to clarify this point (also this dependency).
6. Given the analogy with the results of Ref. S5 (in Supp. Mat.), I would ask the authors to briefly comment on analogies and differences between their proposal and the standard system in which, through proper time-dependent couplings, a single excitation can be deterministically transferred between different atoms. What could be an advantage of using the proposed setup (if there is any)?

Minor comments

7. There are some typos: "direcional" on page 3, G_2 on Fig 4 caption etc.